Journal of Applied Analysis and Computation
Volume 17, Number 2, April 2027, 788–816
Website:http://www.jaac-online.com
DOI:10.11948/20250139

GLOBAL BIFURCATION ANALYSIS OF A PREDATOR-PREY SYSTEM WITH HARVESTING AND STOCKING

Yue Yang[1,2], Yancong Xu[3,†] and Libin Rong[4]

Abstract Predator-prey interactions play a fundamental role in ecological dynamics and are often influenced by external factors such as harvesting and stocking. Understanding how these interventions impact population stability and oscillatory behavior is crucial for effective resource management and conservation efforts. In this paper, we investigate a two-species Leslie predator-prey model incorporating constant-yield harvesting and stocking terms for both species. Through a detailed bifurcation analysis, we unveil the mechanisms behind the suppression or persistence of multiple oscillations in the system. We demonstrate that the model, under harvesting or stocking, exhibits cusp bifurcations of codimension 2 and 3, leading to a rich sequence of bifurcations, including saddle-node bifurcation, Bogdanov-Takens bifurcation of codimension 2 and 3, and Hopf bifurcation of codimension at least 3. In particular, we focus on the role of the conversion rate and analyze its influence on the system's transition between oscillatory and non-oscillatory coexistence states. Our findings suggest that indiscriminate stocking or harvesting of both species is not necessarily beneficial for population persistence; rather, appropriate management strategies should be designed according to specific parameter conditions. Finally, numerical simulations, including bifurcation diagrams and phase portraits, are presented, which provide valuable insights and potential applications in ecological management and conservation biology.

Keywords Harvesting and stocking, cusp of codimension 2 and 3, saddle-node bifurcation, Bogdanov-Takens bifurcation of codimension 2 and 3, Hopf bifurcation of codimension 3.

MSC(2010) 37G05, 37G10, 37G15, 37N25.

1. Introduction

Over the past few decades, the dynamics of harvested populations have attracted considerable attention from researchers [4, 6, 8, 10, 14, 16, 18, 24, 26–29, 31], as predation is a fundamental interaction in biological systems, and harvesting is widely practiced in fisheries, forestry, and wildlife management. Several common types of harvesting have been studied, including constant-effort harvesting and constant-yield harvesting, which were proposed by May et al. [18]. These approaches are expressed, respectively, as a constant proportion of the population under harvest and a constant independent of the population size. Another approach, seasonal harvesting, represented by a periodic function, was investigated by Liu et al. [17].

[†]The corresponding author.
[1]School of Mathematics and Systems Science, Wuhan University of Science and Technology, 430065 Wuhan, China
[2]School of Mathematics and Statistics, Wuhan University, 430072 Wuhan, China
[3]College of Sciences, China Jiliang University, 310018 Hangzhou, China
[4]Department of Mathematics, University of Florida, 32611 Gainesville, USA
Email: yuey_cn@163.com(Y. Yang), Yancongx@cjlu.edu.cn(Y. Xu), libinrong@ufl.edu(L. Rong)

One of the classic models is the Gause-type predator-prey model with constant-yield harvesting, given by:

$$\frac{dx}{dt} = rx(1-\frac{x}{k}) - a\phi(x)y - h,$$
$$\frac{dy}{dt} = y(-d + ma\phi(x)) - g, \tag{1.1}$$

where $x(t)$ and $y(t)$ represent the densities of prey and predators at time t, respectively. The parameters r, k, a, d, and m are positive constants. The prey population grows with an intrinsic rate r and a carrying capacity k in the absence of predators. a, d, and m denote the predator's capturing rate, death rate, and conversion rate, respectively. h and g represent stocking (negative values) or harvesting (positive values) of prey and predators, respectively.

The functional response $\phi(x)$ describes the rate at which predators consume prey as prey density varies, depending on factors such as prey availability, predator behavior, and environmental conditions. System (1.1) with a Holling type-I response was analyzed by Dai and Tang [8], who studied a scenario where two interacting species are harvested at constant rates. Their results show that the maximum safe harvest is likely to be much smaller than what would be predicted from a local equilibrium analysis and that complex dynamics, such as homoclinic orbits and multiple limit cycles, may arise. For the Holling type-II response $\phi(x) = \frac{x}{a+x}$, where $a > 0$ is the half-saturation constant, system (1.1) with constant-rate harvesting or stocking has been widely examined [3, 5, 11, 12, 19, 20, 22]. When $h = g = 0$, Hsu [12] established two global stability criteria for a locally stable equilibrium. When $h = 0$, Brauer and Soudack [3] investigated the global behavior of system (1.1) and classified stability regions using numerical simulations. Later, Xiao and Ruan [25] showed that system (1.1) with constant-rate predator harvesting has a cusp of codimension 2 and passes through a Bogdanov-Takens bifurcation. Similar analyses were conducted by Brauer and Soudack [3] for $g = 0$ and by Brauer and Soudack [5] in the presence of constant-rate harvesting and/or stocking of both species. Peng et al. [20] examined the Holling type-II response with constant-rate prey harvesting and found that the model can exhibit up to three equilibria in the first quadrant and exhibit several bifurcations, including saddle-node, Bogdanov-Takens of codimension 3, supercritical and subcritical Hopf, and generalized Hopf bifurcations. Myerscough et al. [19] extended prior work [3, 5] to the harvested Rosenzweig-MacArthur model, analyzing the effects of harvesting and stocking rates and prey carrying capacity. Hogarth et al. [11] developed a method to determine the period and the ratio of predator-prey population amplitudes for nearly elliptic limit cycles under constant-rate harvesting and stocking. More recently, Sarif and Sarwardi [22] identified a Bogdanov-Takens bifurcation of codimension 2 in a Gause-type model (1.1) with constant harvesting of both species and delay effects.

System (1.1) with a generalized Holling type-III functional response $\phi(x) = \frac{mx^2}{ax^2+bx+1}$ and prey harvesting was examined by Etoua and Rousseau [10], who showed that the model experiences saddle-node bifurcation, Hopf bifurcations of codimension 1 and 2, heteroclinic bifurcation, and nilpotent saddle bifurcations of codimension 2 and 3. They conjectured that when $b = 0$, the nilpotent saddle reaches infinite codimension and the Hopf bifurcation of order 2 degenerates into a Hopf bifurcation of infinite codimension, which was later proven by Laurin and Rousseau [14]. When $g = 0$, Xiao and Jennings [24] demonstrated that ratio-dependent predator-prey models exhibit rich dynamics, including saddle-node bifurcations, supercritical and subcritical Hopf bifurcations, Bogdanov-Takens bifurcations, and homoclinic and heteroclinic bifurcations.

In this paper, we incorporate both harvesting and stocking while focusing on the effect of conversion rate on species coexistence in a simplified predator-prey model by setting $\phi(x) = x$:

$$\begin{aligned}\frac{dx}{dt} &= rx(1 - \frac{x}{k}) - axy - h,\\ \frac{dy}{dt} &= y(-d + max) - g,\end{aligned} \tag{1.2}$$

where all parameters retain their meanings from system (1.1). Notably, h and g may take negative values, representing stocking rather than harvesting.

Despite extensive studies on predator-prey models, few have explicitly examined the effect of conversion rate, with an exception being Chen et al. [7]. In this paper, we investigate how conversion rate influences species coexistence and the underlying mechanisms of harvesting and stocking. We find that a low conversion rate may lead to system collapse, while an increasing conversion rate can promote long-term species persistence. Additionally, we clarify the influence of harvesting and stocking on system stability and bifurcations, revealing distinct regions where species coexistence is feasible.

The rest of this paper is organized as follows. Section 2 analyzes the existence and classification of equilibria, including cusp points of codimension 2 and 3. Section 3 presents bifurcation analyses, including Bogdanov-Takens bifurcation of codimension 2 and 3 and Hopf bifurcation of codimension 3. Section 4 provides numerical simulations, including bifurcation diagrams and phase portraits. Finally, the paper concludes with a discussion.

2. The existence and type of the equilibria in system (1.2)

Note that when we take $h = g = 0$, system (1.2) has two boundary equilibria $E_0(0, 0)$ and $E_k(k, 0)$. However, when $h \neq 0$ and $g \neq 0$, only positive equilibria remain. Since the analytical process for stocking ($h < 0$ or $g < 0$) is similar to that for harvesting ($h > 0$ or $g > 0$), we focus on the existence and type of equilibria of system (1.2) for $h > 0$ or $g > 0$ for simplicity.

2.1. The existence of the positive equilibria

A positive equilibrium $E(x, y)$ for system (1.2) must satisfy

$$\begin{aligned}&rx(1 - \frac{x}{k}) - axy - h = 0,\\ &maxy - dy - g = 0.\end{aligned} \tag{2.1}$$

From the first equation, we obtain the vertical coordinate of $E(x, y)$ as $y = \frac{-rx^2+krx-hk}{akx}$. To ensure the positivity of y, we require that $h < \frac{kr}{4}$ and $\max\{0, \frac{kr-\sqrt{kr(kr-4h)}}{2r}\} < x < \frac{kr+\sqrt{kr(kr-4h)}}{2r}$. Substituting this y into the second equation of (2.1), we find that x satisfies the cubic equation

$$p(x) \doteq x^3 + p_2x^2 + p_1x + p_0 = 0, \tag{2.2}$$

where $p_2 = -\frac{akm+d}{am}$, $p_1 = \frac{k(a(g+hm)+dr)}{amr}$, $p_0 = -\frac{dkh}{amr}$.

Thus, the existence of positive equilibria in system (1.2) reduces to analyzing the positive roots of equation (2.2) within the interval $(\hat{x}_1,\ \hat{x}_2)$, where $\hat{x}_1 \doteq \max\{0, \frac{kr-\sqrt{kr(kr-4h)}}{2r}\}$ and $\hat{x}_2 \doteq \frac{kr+\sqrt{kr(kr-4h)}}{2r}$. We now examine the cases where equation (2.2) has at most 3 positive roots.

The derivative of $p(x)$ is given by $p'(x) = 3x^2 + 2p_2x + p_1$ and its discriminant is $\Delta = 4p_2^2 - 12p_1$. We analyze two main cases:

When $\Delta \leq 0$, since $p'(x) \geq 0$, the function $p(x)$ is monotonically increasing. This implies that equation (2.2) has a unique positive root in the interval $(\hat{x}_1, \hat{x}_2)$ if $p(\hat{x}_1) < 0,\ p(\hat{x}_2) > 0$. Conversely, there is no positive root if either $p(\hat{x}_1) \geq 0$ or $p(\hat{x}_1) < 0,\ p(\hat{x}_2) \leq 0$.

When $\Delta > 0$, the equation $p'(x) = 0$ has two real roots, denoted as $\tilde{x}_1 = \frac{-p_2-\sqrt{p_2^2-3p_1}}{3}$ and $\tilde{x}_2 = \frac{-p_2+\sqrt{p_2^2-3p_1}}{3}$. Based on the positions of $\tilde{x}_1$ and $\tilde{x}_2$, we analyze the distribution of positive roots of the equation $p(x) = 0$ within the interval $x \in (\hat{x}_1, \hat{x}_2)$ in the following five cases.

Case I. $\hat{x}_2 \leq \tilde{x}_1$ or $\hat{x}_1 \geq \tilde{x}_2$. In this case, since $p'(x) > 0$ for $x \in (\hat{x}_1, \hat{x}_2)$, it follows that $p(x)$ is a monotonically increasing function over this interval. Thus, the same conclusion as in the case $\Delta \leq 0$ holds.

Table 1. The distribution of positive roots of $p(x) = 0$ in the interval $(\hat{x}_1, \hat{x}_2)$ when $\hat{x}_1 < \tilde{x}_1 < \hat{x}_2 \leq \tilde{x}_2$.

Signs of $p(\hat{x}_1), p(\hat{x}_2)$ and $p(\tilde{x}_1)$			Existence of positive roots of $p(x) = 0, x \in (\hat{x}_1, \hat{x}_2)$
$p(\hat{x}_1) \geq 0$	$p(\hat{x}_2) < 0$		a unique positive root, denoted by x_2
	$p(\hat{x}_2) \geq 0$		no positive root
$p(\hat{x}_1) < 0$	$p(\tilde{x}_1) < 0$		no positive root
	$p(\tilde{x}_1) = 0$		one positive root of multiplicity 2, denoted by $\tilde{x}_1 = x_{1,2}$
	$p(\tilde{x}_1) > 0$	$p(\hat{x}_2) < 0$	two positive roots, denoted by $x_1 < x_2$
		$p(\hat{x}_2) \geq 0$	a unique positive root, denoted by x_1

Case II. $\hat{x}_1 < \tilde{x}_1 < \hat{x}_2 \leq \tilde{x}_2$. In this case, $p(x)$ first increases monotonically in the interval $(\hat{x}_1, \tilde{x}_1)$, then decreases monotonically in the interval $(\tilde{x}_1, \hat{x}_2)$. A simple analysis summarizes the existence of positive roots of $p(x) = 0$ for $x \in (\hat{x}_1, \hat{x}_2)$, as shown in Table 1.

Table 2. The distribution of positive roots of $p(x) = 0, x \in (\hat{x}_1, \hat{x}_2)$ when $\hat{x}_1 < \tilde{x}_1 < \tilde{x}_2 < \hat{x}_2$ and $p(\hat{x}_1) \geq 0$.

Signs of $p(\tilde{x}_2)$ and $p(\hat{x}_2)$		Existence of positive roots of $p(x) = 0, x \in (\hat{x}_1, \hat{x}_2)$
$p(\tilde{x}_2) < 0$	$p(\hat{x}_2) > 0$	two positive roots, labeled as $x_2 < x_3$
	$p(\hat{x}_2) \leq 0$	a unique positive root, labeled as x_2
$p(\tilde{x}_2) = 0$		one positive root of multiplicity 2, labeled as $\tilde{x}_2 = x_{2,3}$
$p(\tilde{x}_2) > 0$		no positive root

Case III. $\hat{x}_1 < \tilde{x}_1 < \tilde{x}_2 < \hat{x}_2$. In this case, $p(x)$ monotonically increases, then monotonically decreases, and finally monotonically increases in the interval $(\hat{x}_1, \tilde{x}_1)$, $(\tilde{x}_1, \tilde{x}_2)$, and $(\tilde{x}_2, \hat{x}_2)$, respectively. Further, according to the sign of $p(\hat{x}_1)$, we can derive that
(i) for $p(\hat{x}_1) \geq 0$, see Table 2;
(ii) for $p(\hat{x}_1) < 0$, see Table 3.

Case IV. $\tilde{x}_1 \leq \hat{x}_1 < \hat{x}_2 \leq \tilde{x}_2$. In this case, $p'(x) < 0$ for $x \in (\hat{x}_1, \hat{x}_2)$, meaning that $p(x)$ is a monotonically decreasing function in the interval $(\hat{x}_1, \hat{x}_2)$. Therefore, the equation $p(x) = 0$ has a unique positive root if $p(\hat{x}_1) > 0,\ p(\hat{x}_2) < 0$, and has no positive root if $p(\hat{x}_1) > 0,\ p(\hat{x}_2) \geq 0$

or $p(\hat{x}_1) \leq 0$.

Case V. $\tilde{x}_1 \leq \hat{x}_1 < \tilde{x}_2 < \hat{x}_2$. In this case, the function $p(x)$ first decreases monotonically in the interval $(\hat{x}_1, \tilde{x}_2)$ and then increases monotonically in the interval $(\tilde{x}_2, \hat{x}_2)$. Based on the signs of $p(\hat{x}_1)$, $p(\hat{x}_2)$ and $p(\tilde{x}_2)$, we determine the distribution of positive roots of $p(x) = 0$ for $x \in (\hat{x}_1, \hat{x}_2)$, as summarized in Table 4.

Table 3. The distribution of positive roots of $p(x)$ in the interval $(\hat{x}_1, \hat{x}_2)$ when $\hat{x}_1 < \tilde{x}_1 < \tilde{x}_2 < \hat{x}_2$ and $p(\hat{x}_1) < 0$.

Signs of $p(\tilde{x}_1), p(\tilde{x}_2)$ and $p(\hat{x}_2)$			Existence of positive roots of $p(x) = 0, x \in (\hat{x}_1, \hat{x}_2)$
$p(\tilde{x}_1) > 0$	$p(\tilde{x}_2) < 0$	$p(\hat{x}_2) > 0$	3 positive roots, denoted by $x_1 < x_2 < x_3$
		$p(\hat{x}_2) \leq 0$	2 positive roots, denoted by $x_1 < x_2$
	$p(\tilde{x}_2) = 0$		2 positive roots, one of them is positive root of multiplicity 2, denoted by $x_1 < \tilde{x}_2 = x_{2,3}$
	$p(\tilde{x}_2) > 0$		a unique positive root, denoted by x_1
$p(\tilde{x}_1) = 0$	$p(\hat{x}_2) > 0$		two positive roots, one of them is a positive root of multiplicity 2, denoted by $\tilde{x}_1 = x_{1,2} < x_3$
	$p(\hat{x}_2) \leq 0$		one positive root of multiplicity 2, denoted by $\tilde{x}_1 = x_{1,2}$
$p(\tilde{x}_1) < 0$	$p(\hat{x}_2) > 0$		a unique positive root, denoted by x_3
	$p(\hat{x}_2) \leq 0$		no positive root

Table 4. The distribution of positive roots of $p(x) = 0, x \in (\hat{x}_1, \hat{x}_2)$ when $\tilde{x}_1 \leq \hat{x}_1 < \tilde{x}_2 < \hat{x}_2$.

Signs of $p(\hat{x}_1), p(\tilde{x}_2)$ and $p(\hat{x}_2)$			Existence of positive roots of $p(x) = 0, x \in (\hat{x}_1, \hat{x}_2)$
$p(\hat{x}_1) \leq 0$		$p(\hat{x}_2) > 0$	a unique positive root, denoted by x_3
		$p(\hat{x}_2) \leq 0$	no positive root
$p(\hat{x}_1) > 0$	$p(\tilde{x}_2) < 0$	$p(\hat{x}_2) > 0$	two positive roots, denoted by $x_2 < x_3$
		$p(\hat{x}_2) \leq 0$	a unique positive root, denoted by x_2
	$p(\tilde{x}_2) = 0$		one positive root of multiplicity 2, denoted by $\tilde{x}_2 = x_{2,3}$
	$p(\tilde{x}_2) > 0$		no positive root

2.2. The type of positive equilibria

As previously analyzed, when the positive roots $x_i, i = 1, 2, 3$ of the equation $p(x) = 0$ for $x \in (\hat{x}_1, \hat{x}_2)$ exist, system (1.2) possesses positive equilibria $E_i(x_i, y_i)$, where $i = 1, 2, 3$. Similarly, if the equation $p(x) = 0$ has a double root $x_{i,i+1}$ for $i = 1, 2$, system (1.2) has the corresponding positive equilibria $E_{i,i+1}(x_{i,i+1}, y_{i,i+1})$. In the following analysis, we focus on determining the type of these positive equilibria.

Let $E(x, y) = E(x, \frac{-rx^2+krx-hk}{akx})$ be any positive equilibrium of system (1.2). The associated variational matrix evaluated at this point can be expressed by

$$\mathrm{J(E)} = \begin{pmatrix} \dfrac{h}{x} - \dfrac{rx}{k} & -ax \\ m(r - \dfrac{h}{x} - \dfrac{rx}{k}) & amx - d \end{pmatrix},$$

and the characteristic equation associated with $J(E)$ is given by

$$\lambda^2 - \mathrm{tr}(\mathrm{J(E)})\lambda + \det(\mathrm{J(E)}) = 0.$$

It follows that

$$\begin{aligned}
\det(\mathrm{J(E)}) &= \frac{-2amrx^3 + r(akm+d)x^2 - dhk}{kx} \\
&= \frac{amr(p(x) - xp'(x))}{kx} \\
&= -\frac{amr}{k}p'(x), \\
\mathrm{tr}(\mathrm{J(E)}) &= amx - d + \frac{h}{x} - \frac{rx}{k} \doteq t(x)
\end{aligned} \tag{2.3}$$

are the determinant and trace of $J(E)$, respectively. From equation (2.3), it follows directly that the sign of $\det(J(E))$ is the opposite of the sign of $p'(x)$. Thus, a straightforward qualitative analysis leads to the following conclusions.

Theorem 2.1. *Assume that $E_i(x_i, y_i)$ $(i = 1, 2, 3)$ is a simple positive equilibrium of system* (1.2)*. We have*
(I) If $p'(x) > 0$, then E_i is a saddle.
(II) If $p'(x) < 0$ and $t(x) < 0$, then E_i is a stable node or focus.
(III) If $p'(x) < 0$ and $t(x) > 0$, then E_i is an unstable node or focus.
Here $p(x)$ and $t(x)$ are defined in equations (2.2) *and* (2.3)*, respectively.*

Remark 2.1. Based on the existence of positive equilibria in system (1.2), we have $p'(x_1) > 0$ and $p'(x_3) > 0$ when system (1.2) possesses three distinct positive equilibria, $E_1(x_1, y_1)$, $E_2(x_2, y_2)$, and $E_3(x_3, y_3)$, with $x_1 < x_2 < x_3$. Consequently, E_1 and E_3 are saddles.

Next, we analyze the type of equilibrium $E_{i,i+1}(x_{i,i+1}, y_{i,i+1})$ for $(i = 1, 2)$ in system (1.2). Since $x_{i,i+1}$ is a double root of the equation $p(x) = 0$, and given the relation (2.3), it follows that $E_{i,i+1}(x_{i,i+1}, y_{i,i+1})$ is a degenerate equilibrium of system (1.2). For convenience, we denote it as $E^*(x^*, y^*) = E^*(x^*, \frac{-rx^{*2}+krx^*-hk}{akx^*})$. Our conclusion is summarized in Theorem 2.2.

Theorem 2.2. *Assume that $p(x^*) = p'(x^*) = 0$ and $p''(x^*) \neq 0$. We have*
(I) If $t(x^*) \neq 0$, then $E^*(x^*, y^*)$ is a saddle-node point.
(II) If $t(x^*) = 0$ and $t'(x^*) \neq 0$, then $E^*(x^*, y^*)$ is a cusp of codimension 2.
(III) If $t(x^*) = t'(x^*) = 0$, then $E^*(x^*, y^*)$ is a cusp of codimension 3.
Here $p(x)$ and $t(x)$ are defined in equations (2.2) *and* (2.3)*, respectively.*

Proof. (i) Firstly, from $p(x^*) = p'(x^*)$ we know that

$$h = \frac{rx^{*2}(am(k-2x^*)+d)}{dk}, \ g = -\frac{r(k-2x^*)(d-amx^*)^2}{adk}.$$

Next, we let $X = x - x^*, Y = y - y^*$, which transforms $E^*(x^*, y^*)$ to the origin. By Taylor expansion, system (1.2) becomes

$$\begin{aligned}
\frac{dx}{dt} &= \hat{a}_{10}x + \hat{a}_{01}y + \hat{a}_{20}x^2 + \hat{a}_{11}xy, \\
\frac{dy}{dt} &= \hat{b}_{10}x + \hat{b}_{01}y + \hat{b}_{11}xy,
\end{aligned} \tag{2.4}$$

where

$$\hat{a}_{10} = \frac{amrx^*(k-2x^*)}{dk},\ \hat{a}_{01} = -ax^*,\ \hat{a}_{20} = -\frac{r}{k},\ \hat{a}_{11} = -a,$$
$$\hat{b}_{10} = \frac{mr(k-2x^*)(d-amx^*)}{dk},\ \hat{b}_{01} = amx^* - d,\ \hat{b}_{11} = am.$$

In view of $\hat{a}_{10} + \hat{b}_{01} = t(x^*) \neq 0$, we let $X = \frac{\hat{b}_{01}x - \hat{a}_{01}y}{\hat{a}_{10}+\hat{b}_{01}}$, $Y = \frac{\hat{a}_{10}x + \hat{a}_{01}y}{\hat{a}_{10}+\hat{b}_{01}}$, $t = \frac{1}{\hat{a}_{10}+\hat{b}_{01}}\tau$. System (2.4) continues as

$$\frac{dx}{dt} = \hat{c}_{20}x^2 + \hat{c}_{11}xy + \hat{c}_{02}y^2,$$
$$\frac{dy}{dt} = y + \hat{d}_{20}x^2 + \hat{d}_{11}xy + \hat{d}_{02}y^2, \tag{2.5}$$

where

$$\hat{c}_{20} = \frac{\hat{a}_{01}\hat{a}_{20}\hat{b}_{01} + \hat{a}_{10}(\hat{a}_{01}\hat{b}_{11} - \hat{a}_{11}\hat{b}_{01})}{\hat{a}_{01}(\hat{a}_{10}+\hat{b}_{01})^2},$$
$$\hat{c}_{11} = \frac{\hat{b}_{01}(\hat{a}_{11}(\hat{b}_{01} - \hat{a}_{10}) + 2\hat{a}_{01}\hat{a}_{20}) + \hat{a}_{01}\hat{b}_{11}(\hat{a}_{10} - \hat{b}_{01})}{\hat{a}_{01}(\hat{a}_{10}+\hat{b}_{01})^2},$$
$$\hat{c}_{02} = \frac{b_{01}(\hat{a}_{11}\hat{b}_{01} + \hat{a}_{01}(\hat{a}_{20} - \hat{b}_{11}))}{\hat{a}_{01}(\hat{a}_{10}+\hat{b}_{01})^2},$$
$$\hat{d}_{20} = -\frac{\hat{a}_{10}(\hat{a}_{01}(\hat{b}_{11} - \hat{a}_{20}) + \hat{a}_{10}\hat{a}_{11})}{\hat{a}_{01}(\hat{a}_{10}+\hat{b}_{01})^2},$$
$$\hat{d}_{11} = \frac{\hat{a}_{10}(\hat{a}_{11}(\hat{b}_{01} - \hat{a}_{10}) + 2\hat{a}_{01}\hat{a}_{20}) + \hat{a}_{01}\hat{b}_{11}(\hat{b}_{01} - \hat{a}_{10})}{\hat{a}_{01}(\hat{a}_{10}+\hat{b}_{01})^2},$$
$$\hat{d}_{02} = \frac{\hat{a}_{10}(\hat{a}_{11}\hat{b}_{01} + \hat{a}_{01}\hat{a}_{20}) + \hat{a}_{01}\hat{b}_{01}\hat{b}_{11}}{\hat{a}_{01}(\hat{a}_{10}+\hat{b}_{01})^2}.$$

By Theorem 7.1 in Zhang et al. [30], we know that $E^*(x^*, y^*)$ is a saddle-node, and there is a parabolic sector on the right (or left) half plane.

(*ii*) From $p(x^*) = p'(x^*) = t(x^*) = 0$, we know that $h = \frac{x^*(d-amx^*)(am(k-2x^*)+d)}{am(k-2x^*)}$, $g = \frac{(amx^*-d)^3}{a^2mx^*}$ and $r = \frac{dk(d-amx^*)}{amx^*(k-2x^*)}$. We make the following transformations

$$X = x - x^*, Y = y - y^*,$$
$$U = X, V = (d - amx^*)X - ax^*Y,$$
$$u = U, v = \frac{dU}{dt}, dt = (1 - \frac{1}{x^*}U)d\tau,$$
$$x = u, y = (1 - \frac{1}{x^*}u)v.$$

System (1.2) can be written as follows (we still denote τ by t)

$$\frac{dx}{dt} = y,$$
$$\frac{dy}{dt} = a^*_{20}x^2 + a^*_{11}xy + o(|x,y|^2),$$

where

$$a_{20}^* = \frac{d(amx^* - d)(am(k - 3x^*) + d)}{amx^*(k - 2x^*)},$$
$$a_{11}^* = \frac{2a^2m^2x^*(2x^* - k) + adm(k - 4x^*) + 2d^2}{amx^*(2x^* - k)} = t'(x^*).$$

Since $p''(x^*) \neq 0$ and $t'(x^*) \neq 0$, we conclude that a_{20}^* and a_{11}^* are both nonzero. Thus, $E^*(x^*, y^*)$ is a cusp of codimension 2. This completes the proof of Theorem 2.2 (ii). Next, we turn to the proof of Theorem 2.2 (iii).

(iii) From $p(x^*) = p'(x^*) = t(x^*) = t'(x^*) = 0$, we know that $h = \frac{dx^*}{2}, g = \frac{(amx^*-d)^3}{a^2mx^*}, r = \frac{2amx^*(amx^*-d)+d^2}{amx^*}$ and $k = \frac{2\left(2amx^*(amx^*-d)+d^2\right)}{am(2amx^*-d)}$. Similar to (ii), let $X = x - x^*, Y = y - y^*$ to shift the positive equilibrium point $E^*(x^*, y^*)$ to the origin and expand the resulting system around the origin. Then, we obtain the following system (for convenience, in subsequent steps, we continue to denote X, Y, and τ as x, y, and t, respectively):

$$\begin{aligned} \frac{dx}{dt} &= (d - amx^*)x - ax^*y + \frac{d - 2amx^*}{2x^*}x^2 - axy, \\ \frac{dy}{dt} &= \frac{(d - amx^*)^2}{ax^*}x + y(amx^* - d) + amxy. \end{aligned} \tag{2.6}$$

Setting $X = x, Y = \frac{dx}{dt}$, we rewrite system (2.6) as

$$\begin{aligned} \frac{dx}{dt} &= y, \\ \frac{dy}{dt} &= a_{20}x^2 + a_{02}y^2 + a_{30}x^3 + a_{21}x^2y + a_{12}xy^2 + a_{31}x^3y + a_{22}x^2y^2 + o(|x, y|^4), \end{aligned} \tag{2.7}$$

where

$$a_{20} = \frac{(amx^* - d)(2amx^* + d)}{2x^*},\ a_{02} = \frac{1}{x^*},\ a_{30} = \frac{am(2amx^* - d)}{2x^*},$$
$$a_{21} = \frac{d}{2x^{*2}},\ a_{12} = -\frac{1}{x^{*2}},\ a_{31} = -\frac{d}{2x^{*3}},\ a_{22} = \frac{1}{x^{*3}}.$$

Introducing $dt = (1 - a_{02}x)d\tau$, and $X = x, Y = (1 - a_{02}x)y$, system (2.7) becomes

$$\begin{aligned} \frac{dx}{dt} &= y, \\ \frac{dy}{dt} &= a_{20}x^2 + (a_{30} - 2a_{02}a_{20})x^3 + a_{21}x^2y + (a_{12} - a_{02}^2)xy^2 + (a_{02}^2a_{20} - 2a_{02}a_{30})x^4 \\ &\quad +(a_{31} - a_{02}a_{21})x^3y + (a_{22} - a_{02}^3)x^2y^2 + o(|x, y|^4). \end{aligned} \tag{2.8}$$

Since $a_{20} = \frac{(amx^*-d)(2amx^*+d)}{2x^*} \neq 0$, by changes of variables and scaling of time $X = \pm x, Y = \pm\frac{y}{\sqrt{\pm a_{20}}}, \tau = \sqrt{\pm a_{20}}t$, system (2.8) can be rewritten as

$$\begin{aligned} \frac{dx}{dt} &= y, \\ \frac{dy}{dt} &= x^2 \pm \frac{a_{30} - 2a_{02}a_{20}}{a_{20}}x^3 + \frac{a_{02}^2a_{20} - 2a_{02}a_{30}}{a_{20}}x^4 + y(\frac{a_{21}}{\sqrt{\pm a_{20}}}x^2 \pm \frac{a_{31} - a_{02}a_{21}}{\sqrt{\pm a_{20}}}x^3) \end{aligned}$$

$$+y^2((a_{12}-a_{02}^2)x \pm (a_{22}-a_{02}^3)x^2) + o(|x,y|^4). \tag{2.9}$$

By Proposition 5.3 in Lamontagne et al. [13], an equivalent form of system (2.9) can be obtained as follows

$$\frac{dx}{dt} = y,$$
$$\frac{dy}{dt} = x^2 + Fx^3y + o(|x,y|^4),$$

where

$$F = \frac{a_{21}(a_{02}a_{20}-a_{30}) + a_{20}a_{31}}{(\pm a_{20})^{\frac{3}{2}}} = \frac{adm(d-2amx^*)}{4(\pm a_{20}^{\frac{3}{2}})x^{*3}} \neq 0.$$

Thus, $E^*(x^*, y^*)$ is a cusp of codimension 3. This completes the proof of Theorem 2.2 (iii). □

3. Bifurcation analysis

3.1. Bogdanov-Takens bifurcation of codimension 2

In this section, we examine whether system (1.2) exhibits a Bogdanov-Takens bifurcation of codimension 2 under small parameter perturbations, given that the bifurcation parameters are appropriately chosen. Specifically, we establish the following result.

Theorem 3.1. *Suppose that $p(x^*) = p'(x^*) = t(x^*) = 0$ with $p''(x^*)$ and $t'(x^*) \neq 0$. Then $E^*(x^*, y^*) = (x^*, \frac{(d-amx^*)^2}{a^2mx^*})$ is a cusp of codimension 2. Furthermore, if we choose h and g as bifurcation parameters and assume that $k \neq \frac{2x^*(2d-amx^*)}{d}$, then system (1.2) undergoes a Bogdanov-Takens bifurcation of codimension 2 in a small neighborhood of E^*. Here $p(x)$ and $t(x)$ are defined in equations (2.2) and (2.3), respectively.*

Proof. From $p(x^*) = p'(x^*) = t(x^*) = 0$, we know that $h = \frac{x^*(d-amx^*)(am(k-2x^*)+d)}{am(k-2x^*)}$, $g = \frac{(amx^*-d)^3}{a^2mx^*}$ and $r = \frac{dk(d-amx^*)}{amx^*(k-2x^*)}$. Choosing h and g as bifurcation parameters yields the following disturbed system

$$\frac{dx}{dt} = rx(1-\frac{x}{k}) - axy - (h+\upsilon_1),$$
$$\frac{dy}{dt} = maxy - dy - (g+\upsilon_2), \tag{3.1}$$

in which $r, k, a, m, d > 0$, h, g are arbitrary nonzero constants and $\upsilon = (\upsilon_1, \upsilon_2) \sim (0,0)$. We focus on analyzing the dynamics of system (1.2) around the positive equilibrium $E^*(x^*, y^*) = (x^*, \frac{(d-amx^*)^2}{a^2mx^*})$.

Letting $X = x - x^*, Y = y - \frac{(d-amx^*)^2}{a^2mx^*}$ to transform the positive equilibrium point $E^*(x^*, \frac{(d-amx^*)^2}{a^2mx^*})$ of system (3.1) when $\upsilon = 0$ into the origin and expanding the resulting system around the origin, we have (for convenience, in every subsequent transformation, we rename X, Y, τ by x, y, t, respectively)

$$\frac{dx}{dt} = -\upsilon_1 + (d-amx^*)x - ax^*y - \frac{d(d-amx^*)}{amx^*(k-2x^*)}x^2 - axy,$$

$$\frac{dy}{dt} = -\upsilon_2 + \frac{(d-amx^*)^2}{ax^*}x + (amx^* - d)y + amxy.$$

Setting $X = x, Y = \frac{dx}{dt}$, we obtain

$$\begin{aligned} \frac{dx}{dt} &= y, \\ \frac{dy}{dt} &= \overline{a}^*_{00} + \overline{a}^*_{10}x + \overline{a}^*_{01}y + \overline{a}^*_{20}x^2 + \overline{a}^*_{11}xy + \overline{a}^*_{02}y^2 + P_1(x, y, \upsilon_1, \upsilon_2), \end{aligned} \tag{3.2}$$

in which

$$\begin{aligned} \overline{a}^*_{00} &= (amx^* - d)\upsilon_1 + ax^*\upsilon_2, \quad \overline{a}^*_{10} = a(m\upsilon_1 + \upsilon_2), \quad \overline{a}^*_{01} = \frac{\upsilon_1}{x^*}, \\ \overline{a}^*_{20} &= \frac{d(amx^* - d)(am(k-3x^*) + d)}{amx^*(k-2x^*)}, \\ \overline{a}^*_{11} &= \frac{x^*(2a^2m^2x^*(2x^*-k) + adm(k-4x^*) + 2d^2) + am(k-2x^*)\upsilon_1}{amx^{*2}(2x^*-k)}, \quad \overline{a}^*_{02} = \frac{1}{x^*}, \end{aligned}$$

and $P_1(x, y, \upsilon_1, \upsilon_2)$ is C^∞ function at least of third order with respect to x, y, whose coefficients depend smoothly on υ_1 and υ_2. We note that $\overline{a}^*_{00} = \overline{a}^*_{10} = \overline{a}^*_{01} = 0$ when $\upsilon = 0$.

Next, we introduce time rescaling $dt = (1 - \overline{a}^*_{02}x)d\tau$ and changes of variables $X = x, Y = (1 - \overline{a}^*_{02}x)y$. System (3.2) continues as

$$\begin{aligned} \frac{dx}{dt} &= y, \\ \frac{dy}{dt} &= \overline{b}^*_{00} + \overline{b}^*_{10}x + \overline{b}^*_{01}y + \overline{b}^*_{20}x^2 + \overline{b}^*_{11}xy + P_2(x, y, \upsilon_1, \upsilon_2), \end{aligned}$$

where

$$\begin{aligned} &\overline{b}^*_{00} = \overline{a}^*_{00}, \quad \overline{b}^*_{10} = \overline{a}^*_{10} - 2\overline{a}^*_{00}\overline{a}^*_{02}, \quad \overline{b}^*_{01} = \overline{a}^*_{01}, \\ &\overline{b}^*_{20} = \overline{a}^*_{00}\overline{a}^{*2}_{02} - 2\overline{a}^*_{10}\overline{a}^*_{02} + \overline{a}^*_{20}, \quad \overline{b}^*_{11} = \overline{a}^*_{11} - \overline{a}^*_{01}\overline{a}^*_{02}, \end{aligned}$$

and $P_2(x, y, \upsilon_1, \upsilon_2)$ is a C^∞ function at least of third order with respect to x, y, whose coefficients depend smoothly on υ_1 and υ_2. We have $\overline{b}^*_{00} = \overline{b}^*_{10} = \overline{b}^*_{01} = 0$ when $\upsilon = 0$.

Transformations $X = x + \frac{\overline{b}^*_{10}}{2\overline{b}^*_{20}}, Y = y$ bring the above model to an equivalent model

$$\begin{aligned} \frac{dx}{dt} &= y, \\ \frac{dy}{dt} &= \overline{c}^*_{00} + \overline{c}^*_{01}y + \overline{c}^*_{20}x^2 + \overline{c}^*_{11}xy + P_3(x, y, \upsilon_1, \upsilon_2), \end{aligned}$$

in which

$$\overline{c}^*_{00} = \overline{b}^*_{00} - \frac{\overline{b}^{*2}_{10}}{4\overline{b}^*_{20}}, \quad \overline{c}^*_{01} = \overline{b}^*_{01} - \frac{\overline{b}^*_{10}\overline{b}^*_{11}}{2\overline{b}^*_{20}}, \quad \overline{c}^*_{20} = \overline{b}^*_{20}, \quad \overline{c}^*_{11} = \overline{b}^*_{11},$$

and $P_3(x, y, \upsilon_1, \upsilon_2)$ is C^∞ function at least of third order with respect to x, y, whose coefficients depend smoothly on υ_1 and υ_2. It is noted that $\overline{c}^*_{00} = \overline{c}^*_{01} = 0$ when $\upsilon = 0$.

Setting $X = \frac{\overline{c}_{11}^{*2}}{\overline{c}_{20}^{*}}x, Y = \frac{\overline{c}_{11}^{*3}}{\overline{c}_{20}^{*2}}y, \tau = \frac{\overline{c}_{20}^{*}}{\overline{c}_{11}^{*}}t$, it concludes that

$$\begin{aligned}\frac{dx}{dt} &= y,\\ \frac{dy}{dt} &= \varphi_1 + \varphi_2 y + x^2 + xy + P_4(x, y, \upsilon_1, \upsilon_2),\end{aligned}$$

in which $P_4(x, y, \upsilon_1, \upsilon_2)$ is C^∞ function at least of third order with respect to x, y, whose coefficients depend smoothly on υ_1 and υ_2, and

$$\varphi_1 = \frac{\overline{c}_{00}^{*}\overline{c}_{11}^{*4}}{\overline{c}_{20}^{*3}}, \quad \varphi_2 = \frac{\overline{c}_{01}^{*}\overline{c}_{11}^{*}}{\overline{c}_{20}^{*}}.$$

A direct calculation with the assistance of Mathematica yields

$$\left|\frac{\partial(\varphi_1, \varphi_2)}{\partial(\upsilon_1, \upsilon_2)}\right|_{\upsilon=0} = -\left.\frac{c_{11}^{*5}}{c_{20}^{*4}}\right|_{\upsilon=0} \cdot \frac{a^2m(2amx^{*2} + d(k - 4x^*))}{2(d - amx^*)(am(k - 3x^*) + d)}.$$

From $p''(x^*) \neq 0$ and $t'(x^*) \neq 0$, we know that $c_{20}^*, c_{11}^* \neq 0$ when $\upsilon = 0$. Combining with $k \neq \frac{2x^*(2d-amx^*)}{d}$, we derive that $\left|\frac{\partial(\varphi_1,\varphi_2)}{\partial(\upsilon_1,\upsilon_2)}\right|_{\upsilon=0} \neq 0$. By the results of Bogdanov [1, 2] and Takens [23], system (1.2) passes through a Bogdanov-Takens bifurcation of codimension 2 when (υ_1, υ_2) changes in a small neighborhood of $(0, 0)$. □

3.2. Bogdanov-Takens bifurcation of codimension 3

In this subsection, we illustrate that system (1.2) may pass through a Bogdanov-Takens bifurcation of codimension 3 under appropriate parameter choices. Before presenting the main results, we first state the relevant definition and properties.

Definition 3.1. The bifurcation that results from unfolding the following normal form of a cusp of codimension 3,

$$\begin{aligned}\frac{dx}{dt} &= y,\\ \frac{dy}{dt} &= x^2 \pm x^3 y,\end{aligned} \tag{3.3}$$

is called a cusp type degenerate Bogdanov-Takens bifurcation of codimension 3.

Property 3.1. A universal unfolding of the normal form (3.3) is expressed by

$$\begin{cases}\dfrac{dx}{dt} = y,\\[2mm] \dfrac{dy}{dt} = \zeta_1 + \zeta_2 y + \zeta_3 xy + x^2 \pm x^3 y + R(x, y, \rho),\end{cases} \tag{3.4}$$

where $\rho = (\rho_1, \rho_2, \rho_3) \sim (0, 0, 0)$, $\frac{D(\zeta_1,\zeta_2,\zeta_3)}{D(\rho_1,\rho_2,\rho_3)} \neq 0$ for a small ρ and

$$R(x, y, \rho) = y^2 O(|x, y|^2) + O(|x, y|^5) + O(\rho)(O(y^2) + O(|x, y|^3)) + O(\rho^2)O(|x, y|). \tag{3.5}$$

Our main result is stated as follows.

Theorem 3.2. *Suppose that* $p(x^*) = p'(x^*) = t(x^*) = t'(x^*) = 0$*, and that* $p''(x^*) \neq 0$*. Then* $E^*(x^*, y^*) = (x^*, \frac{(d-amx^*)^2}{a^2mx^*})$ *is a cusp of codimension 3. Moreover, if we choose* (h, m, g) *as bifurcation parameters and assume that* $d \neq \sqrt{2}amx^*$*, then model* (1.2) *undergoes a Bogdanov-Takens bifurcation of codimension 3 in a small neighborhood of* E^**. Here* $p(x)$ *and* $t(x)$ *are defined in equations* (2.2) *and* (2.3)*, respectively.*

Proof. Selecting h, m and g as bifurcation parameters, we get the following system

$$\begin{aligned} \frac{dx}{dt} &= rx(1 - \frac{x}{k}) - axy - (h + \omega_1), \\ \frac{dy}{dt} &= (m + \omega_2)axy - dy - (g + \omega_3), \end{aligned} \tag{3.6}$$

where $\omega = (\omega_1, \omega_2, \omega_3) \sim (0, 0, 0)$.

Next, we transform the positive equilibrium $E^*(x^*, \frac{(d-amx^*)^2}{a^2mx^*})$ of system (3.6) when $\omega = 0$ into the origin by setting $X = x - x^*, Y = y - \frac{(d-amx^*)^2}{a^2mx^*}$ and by the Taylor expansion. System (3.6) continues as (for convenience, in every subsequent transformation, we rename X, Y and τ as x, y and t, respectively)

$$\begin{cases} \dfrac{dx}{dt} = \overline{a}_{00} + \overline{a}_{10}x + \overline{a}_{01}y + \overline{a}_{20}x^2 + \overline{a}_{11}xy, \\ \dfrac{dy}{dt} = \overline{b}_{00} + \overline{b}_{10}x + \overline{b}_{01}y + \overline{b}_{11}xy, \end{cases} \tag{3.7}$$

where $\overline{a}_{ij}, \overline{b}_{ij}$ and all the coefficients involved below are given in **Appendix A**. Notably, $\overline{a}_{00} = \overline{b}_{00} = 0$ when $\omega = 0$.

Letting

$$X = x, \ Y = \frac{dx}{dt},$$

system (3.7) can be rewritten as follows

$$\begin{aligned} \frac{dx}{dt} &= y, \\ \frac{dy}{dt} &= \overline{c}_{00} + \overline{c}_{10}x + \overline{c}_{01}y + \overline{c}_{20}x^2 + \overline{c}_{11}xy + \overline{c}_{02}y^2 + \overline{c}_{30}x^3 + \overline{c}_{21}x^2y + \overline{c}_{12}xy^2 \\ &\quad + \overline{c}_{31}x^3y + \overline{c}_{22}x^2y^2 + o(|x, y|^4). \end{aligned} \tag{3.8}$$

We note that $\overline{c}_{00} = \overline{c}_{10} = \overline{c}_{01} = \overline{c}_{11} = 0$ when $\omega = 0$.

Now, we aim to transform system (3.8) into the form (3.4) to demonstrate the existence of a Bogdanov-Takens bifurcation of codimension 3 by following the seven-step procedure outlined by Li et al. [15].

(I) Removing the y^2-term from system (3.8) when $\omega = 0$. Letting $x = X + \frac{\overline{c}_{02}}{2}X^2, y = Y + \overline{c}_{02}XY$, we can rewrite system (3.8) as

$$\begin{aligned} \frac{dx}{dt} &= y, \\ \frac{dy}{dt} &= \overline{d}_{00} + \overline{d}_{10}x + \overline{d}_{01}y + \overline{d}_{20}x^2 + \overline{d}_{11}xy + \overline{d}_{30}x^3 + \overline{d}_{21}x^2y + \overline{d}_{12}xy^2 \end{aligned}$$

$$+\overline{d}_{40}x^4+\overline{d}_{31}x^3y+\overline{d}_{22}x^2y^2+o(|x,y|^4), \tag{3.9}$$

where $\overline{d}_{00}=\overline{d}_{10}=\overline{d}_{01}=\overline{d}_{11}=0$ when $\omega=0$.

(II) Removing the xy^2-term in system (3.9) when $\omega=0$. Making variables transformation $x=X+\frac{\overline{d}_{12}}{6}X^3, y=Y+\frac{\overline{d}_{12}}{2}X^2Y$, we have

$$\begin{aligned}\frac{dx}{dt}&=y,\\ \frac{dy}{dt}&=\overline{e}_{00}+\overline{e}_{10}x+\overline{e}_{01}y+\overline{e}_{20}x^2+\overline{e}_{11}xy+\overline{e}_{30}x^3+\overline{e}_{21}x^2y+\overline{e}_{40}x^4\\ &\quad+\overline{e}_{31}x^3y+\overline{e}_{22}x^2y^2+o(|x,y|^4),\end{aligned} \tag{3.10}$$

in which $\overline{e}_{00}=\overline{e}_{10}=\overline{e}_{01}=\overline{e}_{11}=0$ when $\omega=0$.

(III) Removing the x^2y^2-term in system (3.10) when $\omega=0$. Let $x=X+\frac{\overline{e}_{22}}{12}X^4$, $y=Y+\frac{\overline{e}_{22}}{3}X^3Y$. System (3.10) becomes

$$\begin{aligned}\frac{dx}{dt}&=y,\\ \frac{dy}{dt}&=\overline{f}_{00}+\overline{f}_{10}x+\overline{f}_{01}y+\overline{f}_{20}x^2+\overline{f}_{11}xy+\overline{f}_{30}x^3+\overline{f}_{21}x^2y+\overline{f}_{40}x^4\\ &\quad+\overline{f}_{31}x^3y+o(|x,y|^4).\end{aligned} \tag{3.11}$$

Note that $\overline{f}_{00}=\overline{f}_{10}=\overline{f}_{01}=\overline{f}_{11}=0$ when $\omega=0$.

(IV) Removing the x^3 and x^4 terms in system (3.11) when $\omega=0$. We know that $\overline{f}_{20}=\frac{(amx^*-d)(2amx^*+d)}{2x^*}+O(\omega)$, $\overline{f}_{20}\neq 0$ for a small ω. It follows from

$$x=X-\frac{\overline{f}_{30}}{4\overline{f}_{20}}X^2+\frac{15\overline{f}_{30}^2-16\overline{f}_{20}\overline{f}_{40}}{80\overline{f}_{20}^2}X^3,\quad y=Y,\quad dt=(1-\frac{\overline{f}_{30}}{2\overline{f}_{20}}X+\frac{45\overline{f}_{30}^2-48\overline{f}_{20}\overline{f}_{40}}{80\overline{f}_{20}^2}X^2)d\tau,$$

that

$$\begin{aligned}\frac{dx}{dt}&=y,\\ \frac{dy}{dt}&=\overline{g}_{00}+\overline{g}_{10}x+\overline{g}_{01}y+\overline{g}_{20}x^2+\overline{g}_{11}xy+\overline{g}_{30}x^3+\overline{g}_{21}x^2y+\overline{g}_{40}x^4\\ &\quad+\overline{g}_{31}x^3y+o(|x,y|^4).\end{aligned} \tag{3.12}$$

We note that $\overline{g}_{00}=\overline{g}_{10}=\overline{g}_{01}=\overline{g}_{11}=\overline{g}_{30}=\overline{g}_{40}=0$ when $\omega=0$.

(V) Removing the x^2y term in system (3.12) when $\omega=0$. We have $\overline{g}_{20}=\frac{(amx^*-d)(2amx^*+d)}{2x^*}+O(\omega)$, $\overline{g}_{20}\neq 0$ for a small ω. Setting

$$x=X,y=Y+\frac{\overline{g}_{21}}{3\overline{g}_{20}}Y^2+\frac{\overline{g}_{21}^2}{36\overline{g}_{20}^2}Y^3,d\tau=(1+\frac{\overline{g}_{21}}{3\overline{g}_{20}}Y+\frac{\overline{g}_{21}^2}{36\overline{g}_{20}^2}Y^2)dt,$$

we get an equivalent system to system (3.12) as follows

$$\begin{aligned}\frac{dx}{dt}&=y,\\ \frac{dy}{dt}&=\overline{h}_{00}+\overline{h}_{10}x+\overline{h}_{01}y+\overline{h}_{20}x^2+\overline{h}_{11}xy+\overline{h}_{31}x^3y+R_1(x,y,\omega),\end{aligned} \tag{3.13}$$

where $\overline{h}_{00} = \overline{h}_{10} = \overline{h}_{01} = \overline{h}_{11} = 0$ when $\omega = 0$, and $R_1(x, y, \omega)$ possesses the property of equation (3.5).

(VI) Changing $\overline{h}_{20}$ and $\overline{h}_{31}$ to 1 in system (3.13). A simple calculation shows that $\overline{h}_{20} = \overline{g}_{20} \neq 0$ and $\overline{h}_{31} \neq 0$ for a small ω. Transformations

$$x = \overline{h}_{20}^{\frac{1}{5}} \overline{h}_{31}^{-\frac{2}{5}} X, \quad y = \overline{h}_{20}^{\frac{4}{5}} \overline{h}_{31}^{-\frac{3}{5}} Y, \quad dt = \overline{h}_{20}^{-\frac{3}{5}} \overline{h}_{31}^{\frac{1}{5}} d\tau,$$

bring the above system to

$$\begin{aligned} \frac{dx}{dt} &= y, \\ \frac{dy}{dt} &= \overline{j}_{00} + \overline{j}_{10}x + \overline{j}_{01}y + \overline{j}_{11}xy + x^2 + x^3y + R_2(x, y, \omega). \end{aligned} \tag{3.14}$$

We have that $\overline{j}_{00} = \overline{j}_{10} = \overline{j}_{01} = \overline{j}_{11} = 0$ when $\omega = 0$, and $R_2(x, y, \omega)$ possesses the property of equation (3.5).

(VII) Removing the $\overline{j}_{10}$ term in system (3.14). Finally, introducing conversion of coordinates

$$x = X - \frac{\overline{j}_{10}}{2}, \quad y = Y,$$

system (3.14) can be expressed as follows

$$\begin{aligned} \frac{dx}{dt} &= y, \\ \frac{dy}{dt} &= \overline{\psi}_1 + \overline{\psi}_2 y + \overline{\psi}_3 xy + x^2 + x^3y + R_3(x, y, \omega), \end{aligned} \tag{3.15}$$

where

$$\overline{\psi}_1 = \overline{j}_{00} - \frac{\overline{j}_{10}^2}{4}, \quad \overline{\psi}_2 = \overline{j}_{01} - \frac{\overline{j}_{10}^3}{8} - \frac{\overline{j}_{11}\overline{j}_{10}}{2}, \quad \overline{\psi}_3 = \overline{j}_{11} + \frac{3\overline{j}_{10}^2}{4}.$$

We get that $\overline{\psi}_1 = \overline{\psi}_2 = \overline{\psi}_3 = 0$ when $\omega = 0$ and $R_3(x, y, \omega)$ possesses the property of equation (3.5). Moreover, with the help of Mathematica, we have

$$\left| \frac{\partial(\overline{\psi}_1, \overline{\psi}_2, \overline{\psi}_3)}{\partial(\omega_1, \omega_2, \omega_3)} \right|_{\omega=0} = \overline{h}_{31}^{\frac{4}{5}} \overline{h}_{20}^{-\frac{12}{5}} |_{\omega=0} \cdot \frac{a(d - 2amx^*)(d^2 - 2a^2m^2x^{*2})}{mx^*(amx^* - d)(2amx^* + d)}.$$

Obviously, we have $\overline{h}_{31}^{\frac{4}{5}} \overline{h}_{20}^{-\frac{12}{5}} |_{\omega=0} \neq 0$. Combining with $d \neq \sqrt{2}amx^*$, we have that $|\frac{\partial(\overline{\psi}_1, \overline{\psi}_2, \overline{\psi}_3)}{\partial(\omega_1, \omega_2, \omega_3)}|_{\omega=0}$ $\neq 0$. Moreover, system (3.15) is precisely in the form of system (3.4). Based on the results of Li et al. [15], we conclude that system (3.15) serves as the universal unfolding of the Bogdanov-Takens singularity (cusp case) of codimension 3. The remainder term $R_3(x, y, \omega)$, which satisfies the property of equation (3.5), does not affect the bifurcation phenomena. Consequently, the dynamics of system (1.2) in a small neighborhood of the positive equilibrium $E^*(x^*, \frac{(d-amx^*)^2}{a^2mx^*})$ as $(\omega_1, \omega_2, \omega_3)$ vary near $(0, 0, 0)$ are equivalent to system (3.15) in a small neighborhood of $(0, 0, 0)$ as $(\overline{\psi}_1, \overline{\psi}_{,2} \overline{\psi}_3)$ vary near $(0, 0, 0)$. This completes the proof. □

3.3. Hopf bifurcation of codimension 3

The existence of equilibria of system (1.2) and equation (2.3) indicate that a Hopf bifurcation may occur around the positive equilibrium $E_2(x_2, y_2)$ due to $\det(J(E_2)) = -\frac{amr}{kx_2}p'(x_2) > 0$. In this subsection, we demonstrate that the degree of degeneration of the Hopf bifurcation can reach at least 3. Our conclusions are as follows.

Theorem 3.3. *Assume that $p(x_2) = t(x_2) = 0$ and $p'(x_2) < 0$. We have*
(I) If $l_1 < 0$, then $E_2(x_2, y_2)$ is a stable weak focus with multiplicity one. Furthermore, a stable limit cycle bifurcates from E_2 via a supercritical Hopf bifurcation.
(II) If $l_1 > 0$, then $E_2(x_2, y_2)$ is an unstable weak focus with multiplicity one. Furthermore, an unstable limit cycle bifurcates from E_2 via a subcritical Hopf bifurcation.
(III) If $l_1 = 0$, then $E_2(x_2, y_2)$ is a weak focus with multiplicity at least two. In this case, system (1.2) *may exhibit a degenerate Hopf bifurcation.*
Here $p(x)$ and $t(x)$ are defined in equations (2.2) *and* (2.3)*, respectively. The coefficient l_1 is given by*

$$l_1 = l_1^2 m^2 + l_1^1 m + l_1^0, \tag{3.16}$$

where $l_1^2 = (dk - kr + 4rx_2)a^2kx_2$, $l_1^1 = (-d^2k^2 + dkr(k - 6x_2) + r^2x_2(k - 4x_2))a$, $l_1^0 = 2dr(dk + rx_2)$.

Proof. It is clear that $h = \frac{x_2(x_2(r-akm)+dk)}{k}$, $g = \frac{(d-amx_2)(-k(amx_2+r)+dk+2rx_2)}{ak}$ due to $p(x_2) = t(x_2) = 0$. Next, letting $X = x - x_2, Y = y - y_2$ and by the Taylor expansion, system (1.2) can be rewritten as (for convenience, we rename X, Y as x, y, respectively)

$$\begin{aligned} \frac{dx}{dt} &= Bx - Qy - \frac{r}{k}x^2 - axy, \\ \frac{dy}{dt} &= Px - By + amxy, \end{aligned} \tag{3.17}$$

where $B = d - amx_2$, $P = \frac{m(k(amx_2+r)-dk-2rx_2)}{k}$ and $Q = ax_2$. A straightforward computation indicates $PQ - B^2 = \frac{d(akmx_2-dk)+amrx_2(k-2x_2)}{k} = x_2 \cdot \det(J(E_2)) > 0$. Letting $\omega = \sqrt{PQ - B^2}$ and making a transformation of $x = QX, y = BX - \omega Y$ and $dt = \frac{1}{\omega}d\tau$, system (3.17) becomes (we still denote X, Y, τ by x, y, t, respectively)

$$\begin{aligned} \frac{dx}{dt} &= y + \frac{a(akmx_2 - dk - rx_2)}{k\omega}x^2 + axy, \\ \frac{dy}{dt} &= -x + \frac{a(amx_2 - d)(dk + rx_2)}{k\omega^2}x^2 + \frac{ad}{\omega}xy. \end{aligned}$$

It follows from the formula in Perko [21] that the first Lyapunov coefficient is

$$L_1 = \frac{a^2x_2l_1}{8k^2\omega^3},$$

in which l_1 is defined as in the equation (3.16). Because a, k, ω and $x_2 > 0$, the sign of L_1 is the same as l_1 and we complete the proof. $\square$

Based on the case (III) of Theorem 3.3, we can conclude that system (1.2) experiences a degenerate Hopf bifurcation around $E_2(x_2, y_2)$ when $l_1 = 0$, i.e., $m = \frac{-l_1^1 \pm \sqrt{(l_1^1)^2 - 4l_1^2 l_1^0}}{2l_1^2}$. A complicated calculation with the assistance of Maple yields the second Lyapunov coefficient as follows:

$$L_2 = \frac{a^5 m x_2^2 l_2}{288 k^5 \omega^7},$$

in which

$$\begin{aligned} l_2 = {} & 20a^4k^3m^4x_2^3(k(d+r)-2rx_2)(dk-kr+4rx_2)+a^3k^2m^3x_2^2(k^2rx_2(-123d^2-344dr \\ & +99r^2)-5k^3(d-r)(11d-r)(d+r)+6kr^2x_2^2(81d-73r)+560r^3x_2^3)+a^2km^2x_2(k^2r^2 \\ & \times x_2^2(-602d^2+907dr-99r^2)+k^3rx_2(122d^3+370d^2r-165dr^2+5r^3)+5dk^4(d-r) \\ & \times(10d-r)(d+r)+2kr^3x_2^3(219r-676d)-560r^4x_2^4)+2dr(3d^3k^4(d+5r)+d^2k^3rx_2 \\ & \times(55r-43d)+dk^2r^2x_2^2(60r-149d)+20kr^3x_2^3(r-7d)-40r^4x_2^4)+am(-15d^5k^5 \\ & -45d^4k^4rx_2+d^3k^3r^2(15k^2-176kx_2+362x_2^2)+d^2k^2r^3x_2(65k^2-575kx_2+1086x_2^2) \\ & +2dkr^4x_2^2(35k^2-251kx_2+402x_2^2)+20r^5x_2^3(k-2x_2)(k-4x_2)), \end{aligned} \tag{3.18}$$

and $m = \frac{-l_1^1 \pm \sqrt{(l_1^1)^2 - 4l_1^2 l_1^0}}{2l_1^2}$. Thus, we can conclude our results in the following theorem.

Theorem 3.4. *Assume that* $p(x_2) = t(x_2) = 0, p'(x_2) < 0$ *and that* $m = \frac{-l_1^1 \pm \sqrt{(l_1^1)^2 - 4l_1^2 l_1^0}}{2l_1^2}$. *We have*
(I) If $l_2 < 0$*, then* $E_2(x_2, y_2)$ *is a stable weak focus with multiplicity 2. System* (1.2) *undergoes a degenerate Hopf bifurcation of codimension 2, and up to two limit cycles can bifurcate from* E_2*, with the outer one being stable.*
(II) If $l_2 > 0$*, then* $E_2(x_2, y_2)$ *is an unstable weak focus with multiplicity 2. System* (1.2) *undergoes a degenerate Hopf bifurcation of codimension 2, and up to two limit cycles can bifurcate from* E_2*, with the outer one being unstable.*
(III) If $l_2 = 0$*, then* $E_2(x_2, y_2)$ *is a weak focus with multiplicity at least three, and system* (1.2) *may undergo a degenerate Hopf bifurcation of codimension at least 3.*
Here $p(x)$*,* $t(x)$*,* l_2*, and* $l_1^i (i = 0, 1, 2)$ *are defined in equations* (2.2), (2.3), (3.18), *and Theorem 3.3, respectively.*

4. Numerical bifurcation results

In this section, we will conduct a detailed numerical bifurcation analysis to validate the theoretical results using the ODE software developed by Doedel et al. [9], with a particular focus on the effect of the conversion rate and the interaction mechanisms of harvesting and stocking for both species. Notably, we consider both harvesting ($h > 0$ and $g > 0$) and stocking ($h < 0$ and $g < 0$) for both species simultaneously.

4.1. m as the primary bifurcation parameter

Firstly, we set the parameter values in system (1.2) as

$$r = 0.4,\ k = 16,\ a = 0.3,\ m = 0.2,\ d = 0.05,\ h = -0.0204,\ g = 0.07, \tag{4.1}$$

and take the conversion rate (m) as the primary bifurcation parameter while keeping the other parameter values fixed as in equation (4.1). Under these conditions, we identify one subcritical

Hopf bifurcation point $HB_1(1.87056, 1.21381)$ at $m = 1.91867 \times 10^{-1}$ and one supercritical Hopf bifurcation point $HB_2(5.74666 \times 10^{-1}, 1.40377)$ at $m = 5.79267 \times 10^{-1}$. Additionally, a saddle-node bifurcation point $SN(9.35065, 5.61384 \times 10^{-1})$ occurs at $m = 6.22743 \times 10^{-2}$.

The first limit cycle branch, which bifurcates from HB_1, has two saddle-node points of limit cycles: $SNC_1(3.39748, 1.66368)$ at $m = 1.91779 \times 10^{-1}$, with a period of 3.37901×10^1; $SNC_2(8.25068, 2.59993)$ at $m = 1.94698 \times 10^{-1}$, with a period of 3.80025×10^1.

The second limit cycle branch, which bifurcates from HB_2, has only one saddle-node point of a limit cycle: $SNC_3(9.81058, 2.92981)$ at $m = 2.04636 \times 10^{-1}$, with a period of 3.97873×10^1.

Both families of limit cycles are approaching their respective homoclinic cycles. Notably, it is evident that an excessively low conversion rate may lead to system collapse. See Figure 1 for details.

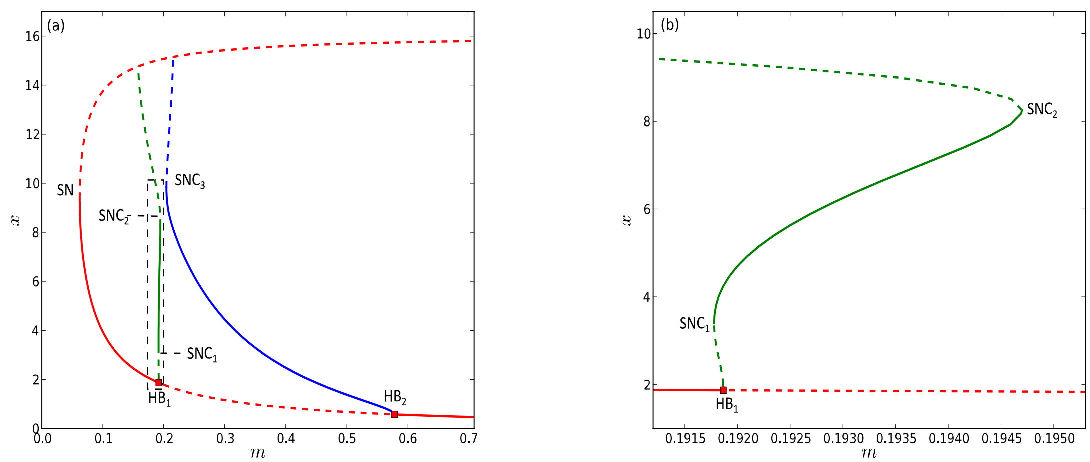

Figure 1. One-parameter bifurcation diagram of system (1.2) with respect to the conversion rate (m). (a) m vs. x. (b) Zoomed-in section of (a).

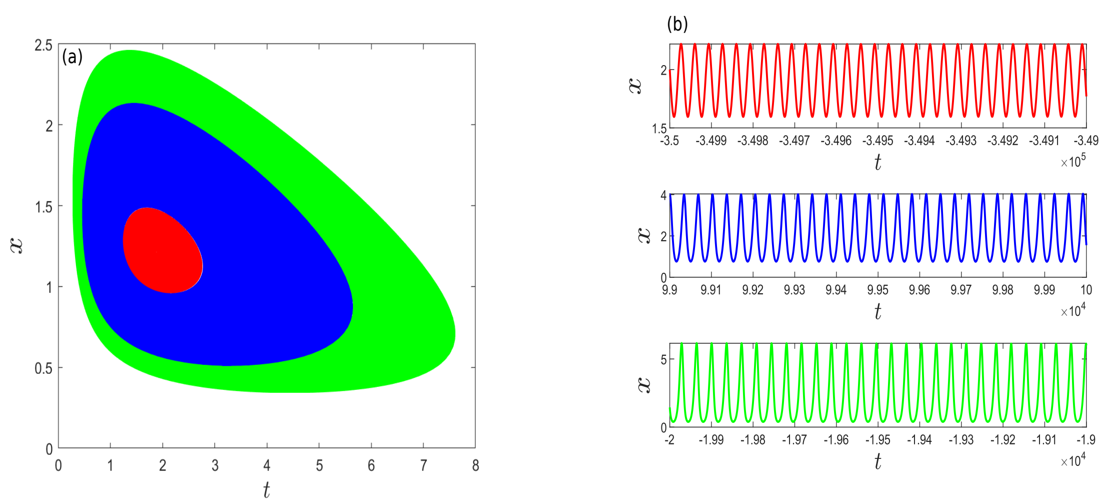

Figure 2. Three limit cycles and their corresponding time evolutions in Figure 1 (b) for $m = 0.190695$. The outermost and innermost cycles are unstable, whereas the middle cycle is stable. (a) Phase portraits of the three limit cycles. (b) Time evolution of the three limit cycles.

4.2. m and h as the primary bifurcation parameters

Next, by setting the conversion rate (m) and the harvesting (or stocking) of the prey (h) as the primary bifurcation parameters while keeping the first set of parameter values in equation (4.1), we obtain the stable (unstable) Hopf bifurcation curve H_s (H_u) (red), saddle-node bifurcation curve SN (blue), homoclinic bifurcation curve Hom (green), and saddle-node bifurcation curve of limit cycles SNL (cyan).

There are three codimension-2 bifurcation points in the system: A Bogdanov-Takens bifurcation point $BT(8.76781, 4.23281\times10^{-1})$ at $m = 8.18809\times10^{-2}, h = 4.71888\times10^{-1}$, a generalized Hopf bifurcation point $GH(1.85746, 1.21569)$ at $m = 1.93060 \times 10^{-1}, h = -2.06994 \times 10^{-2}$, and a codimension-2 cusp of limit cycle bifurcation point $CPL(1.88668, 1.22691)$ at $m = 1.93221 \times 10^{-1}, h = -2.07389 \times 10^{-2}$ with period 3.31502×10^{1}. See Figure 3 (a, b, c, d).

The saddle-node bifurcation curve of limit cycles SNL is shown in Figure 3 (a), where an acute-angled region appears, representing a parameter space where three limit cycles coexist; the outermost and innermost cycles are unstable, whereas the middle cycle is stable. The full bifurcation diagram divides the parameter space into eight regions (I-VIII), with the corresponding phase portraits described as follows (See Figure 4 for details):

Region I: No positive equilibrium.
Region II: A saddle and a stable focus.
Region III: A saddle and an unstable limit cycle containing a stable focus.
Region IV: A saddle and an unstable focus.
Region V: A saddle and a stable limit cycle containing an unstable focus.
Region VI: A saddle and a stable limit cycle enclosing an unstable focus.
Region VII: A saddle, a large unstable limit cycle containing a small stable limit cycle enclosing an unstable focus.
Region VIII: A saddle and three limit cycles-a large unstable limit cycle enclosing a middle stable limit cycle, which in turn encloses a small unstable limit cycle containing a stable focus.

Maintaining a certain level of harvesting or stocking can be beneficial for the biological system by promoting the oscillatory coexistence of both species. However, an excessively high conversion rate (m) and intense harvesting of prey (h) can have a significant negative impact on prey populations and may lead to system collapse.

4.3. m and g as the primary bifurcation parameters

Next, setting the conversion rate (m) and the harvesting (or stocking) of the predator (g) as the primary bifurcation parameters and using the first set of parameter values in equation (4.1), we obtain a two-parameter bifurcation diagram, which includes the supercritical or subcritical Hopf bifurcation curve $H_s(H_u)$ (red), the saddle-node bifurcation curve SN (blue), the homoclinic bifurcation curve Hom (green), and the saddle-node bifurcation curve of limit cycles SNL (cyan). There is one Bogdanov-Takens (BT) bifurcation point $BT(8.81665, 6.06325 \times 10^{-1})$ at $m = 1.03112 \times 10^{-1}$, $g = 1.35047 \times 10^{-1}$, one generalized Hopf bifurcation point $GH(1.84726, 1.21621)$ at $m = 1.93485 \times 10^{-1}, g = 6.95972 \times 10^{-2}$, and one codimension-2 cusp of limit cycle $CPL(5.55448, 2.10949)$ at $m = 1.89732 \times 10^{-1}, g = 7.04308 \times 10^{-2}$, with period 3.54154×10^{1}, indicating the coexistence of three limit cycles (the outermost and innermost cycles are unstable, whereas the middle cycle is stable). See Figure 5 for illustration.

The whole bifurcation diagram is divided into seven regions: I-VII, with the corresponding phase portraits described as follows (See Figure 6 for details):

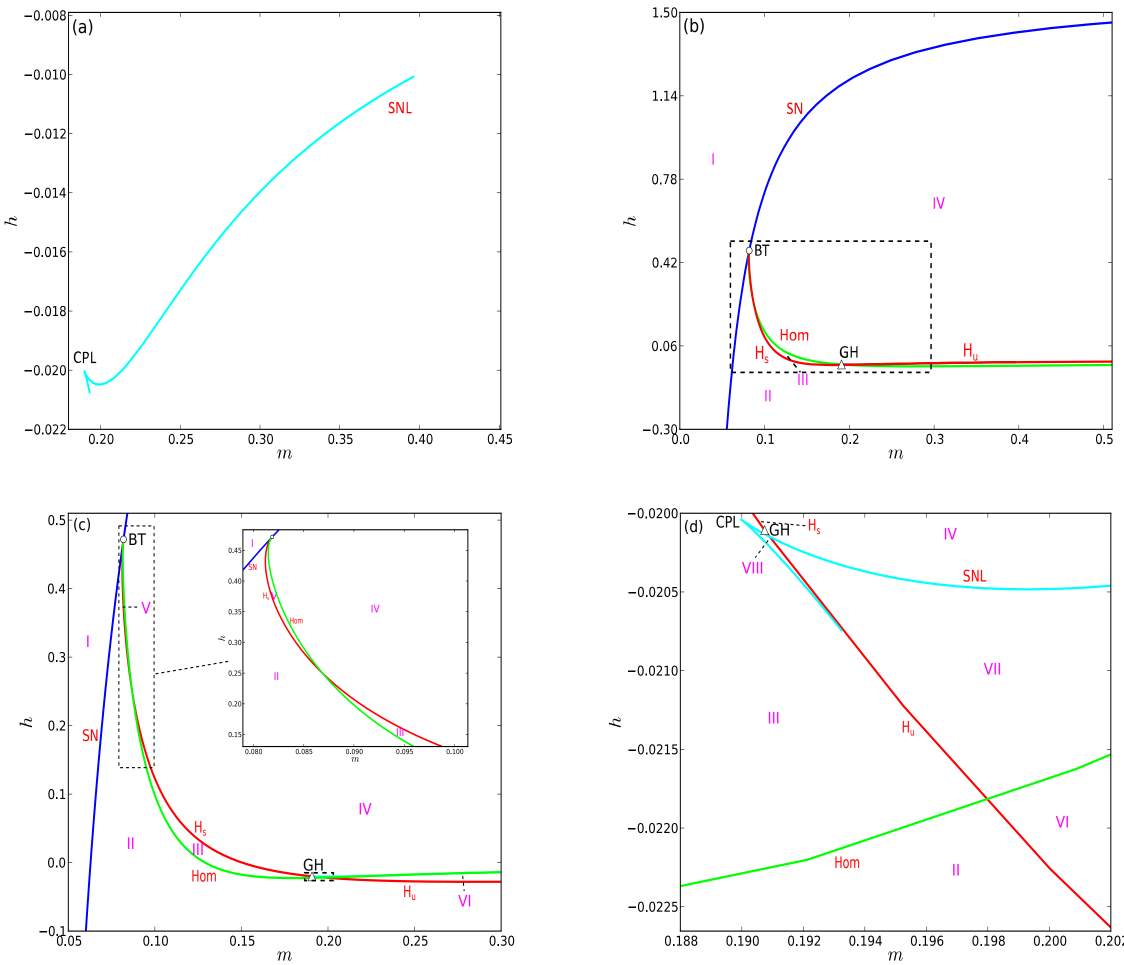

Figure 3. Two-parameter bifurcation diagram of system (1.2) with respect to the conversion rate (m) and the harvesting of the prey (h). (a) The saddle-node bifurcation curve of a limit cycle SNL with a codimension-2 cusp of a limit cycle CPL. (b) m vs. h. (c) First zoomed part of (b). (d) Second zoomed part of (b). Here, SN, H_s (H_u), Hom, SNL, CPL, GH, and BT denote the saddle-node bifurcation curve (blue), stable (unstable) Hopf bifurcation curve (red), homoclinic cycle bifurcation curve (green), saddle-node bifurcation curve of a limit cycle (cyan), cusp of a limit cycle, generalized Hopf bifurcation point, and Bogdanov-Takens bifurcation point, respectively.

Region I: No positive equilibrium.
Region II: A saddle and a stable focus.
Region III: A saddle and an unstable limit cycle enclosing a stable focus.
Region IV: A saddle and an unstable focus.
Region V: A saddle and a stable limit cycle enclosing an unstable focus.
Region VI: A saddle and a large unstable limit cycle enclosing a small stable limit cycle that encloses an unstable hyperbolic positive equilibrium.
Region VII: A saddle and three limit cycles (a large unstable limit cycle encloses a middle stable limit cycle, which in turn encloses a small unstable limit cycle) enclosing a stable hyperbolic positive equilibrium.

When the prey is in the stocking state ($h = -0.0204$), implementing predator harvesting

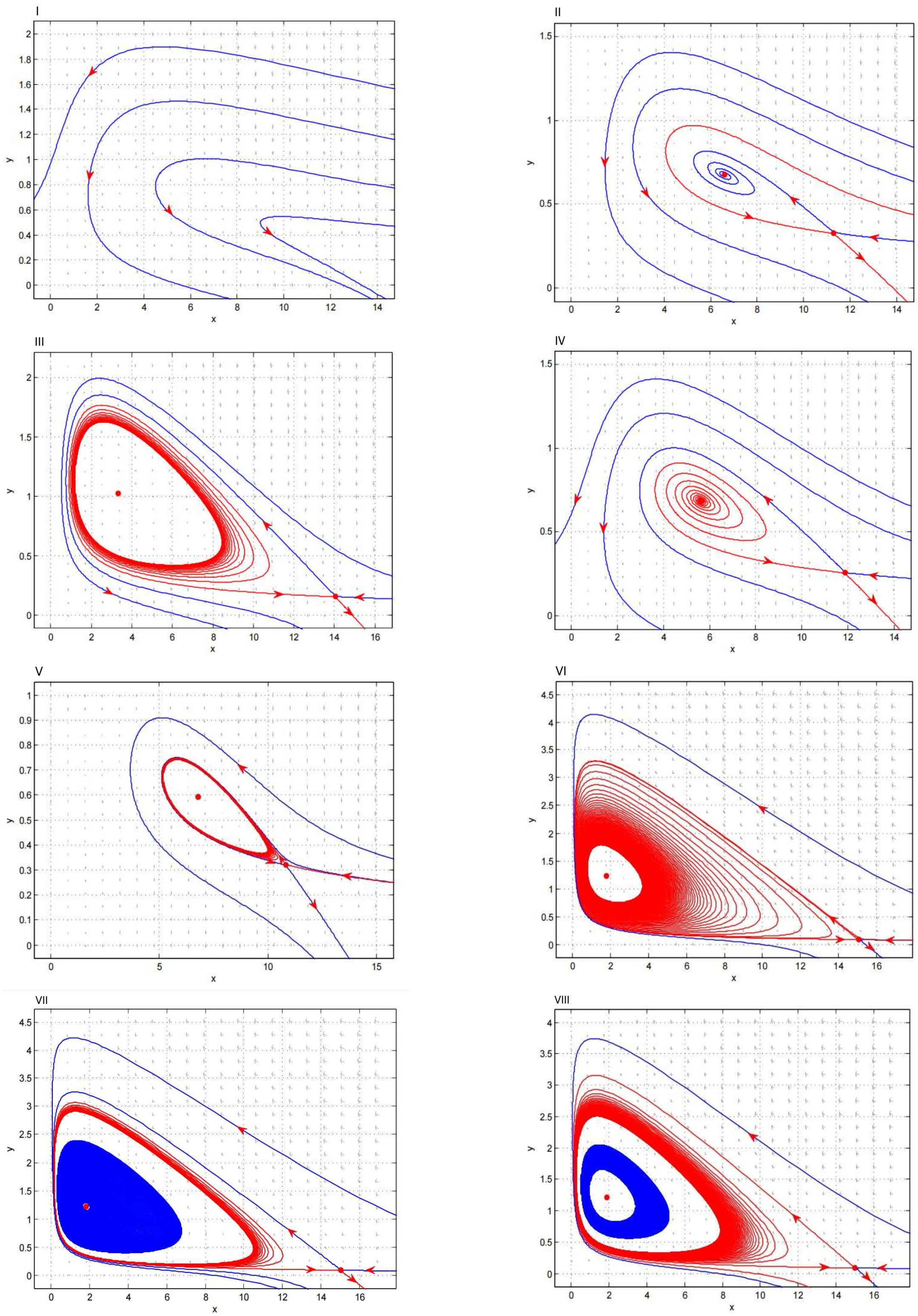

Figure 4. The corresponding phase portraits in regions I-VIII of Figure 3.

benefits the system. However, we find that excessive predator harvesting may lead to system collapse if the conversion rate is too low.

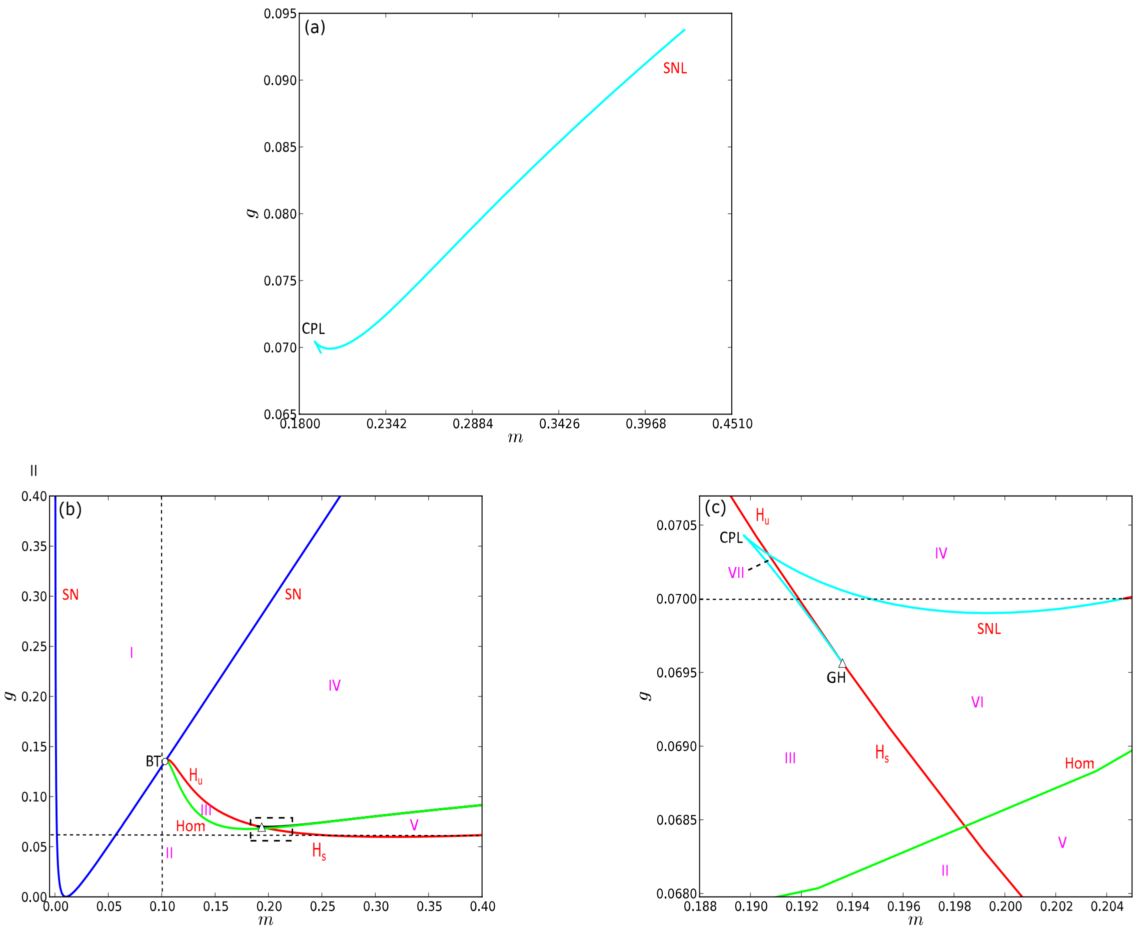

Figure 5. Two-parameter bifurcation diagram of system (1.2) with respect to the conversion rate (m) and the harvesting of the predator (g). (a) The saddle-node bifurcation curve of a limit cycle SNL with a codimension-2 cusp of a limit cycle CPL. (b) m vs. g. (c) Zoomed part of (b). Here, SN, H_s (H_u), Hom, SNL, CPL, GH, and BT denote the saddle-node bifurcation curve (blue), stable (unstable) Hopf bifurcation curve (red), homoclinic cycle bifurcation curve (green), saddle-node bifurcation curve of a limit cycle (cyan), cusp of a limit cycle, generalized Hopf bifurcation point, and Bogdanov-Takens bifurcation point, respectively.

4.4. h as the primary bifurcation parameter

Setting the death rate of the predator as $d = 0.0535$ while keeping the other parameter values unchanged in equation (4.1), we take the stocking or harvesting term of the prey (h) as the primary bifurcation parameter. Under these conditions, we obtain one subcritical Hopf bifurcation point $HB(1.85056, 1.21669)$ at $h = -2.08548 \times 10^{-2}$, one saddle-node bifurcation point $SN(8.11948, 1.61414 \times 10^{-1})$ at $h = 1.20647$, and two saddle-node bifurcation points of limit cycles: $SNC_1(3.89551, 1.81040)$ at $h = -2.09113 \times 10^{-2}$ with period 3.35494×10^{1}, and $SNC_2(7.12654, 2.44896)$ at $h = -2.08043 \times 10^{-2}$ with period 3.62913×10^{1}.

There exists a region with three coexisting limit cycles for $-2.08548 \times 10^{-2} < h < -2.08043 \times 10^{-2}$: The outermost and innermost cycles are unstable, whereas the middle cycle is stable. See

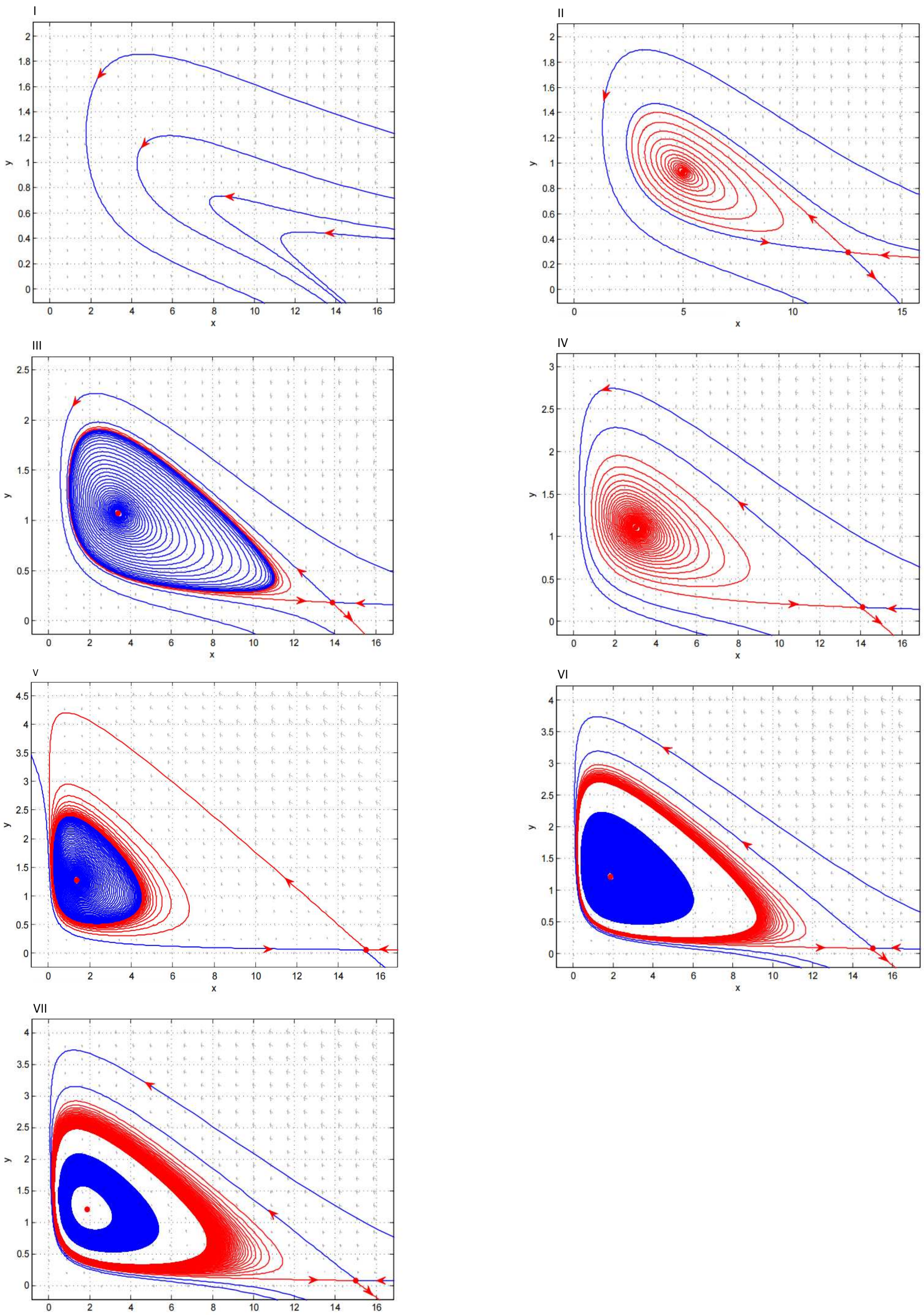

Figure 6. The corresponding phase portraits for regions I-VII in Figure 5.

Figure 7 for details. Notably, the S-type bifurcation branch of the limit cycle suggests the existence of a codimension-2 cusp of limit cycles. It is evident that an excessively high level of prey harvesting may lead to system collapse.

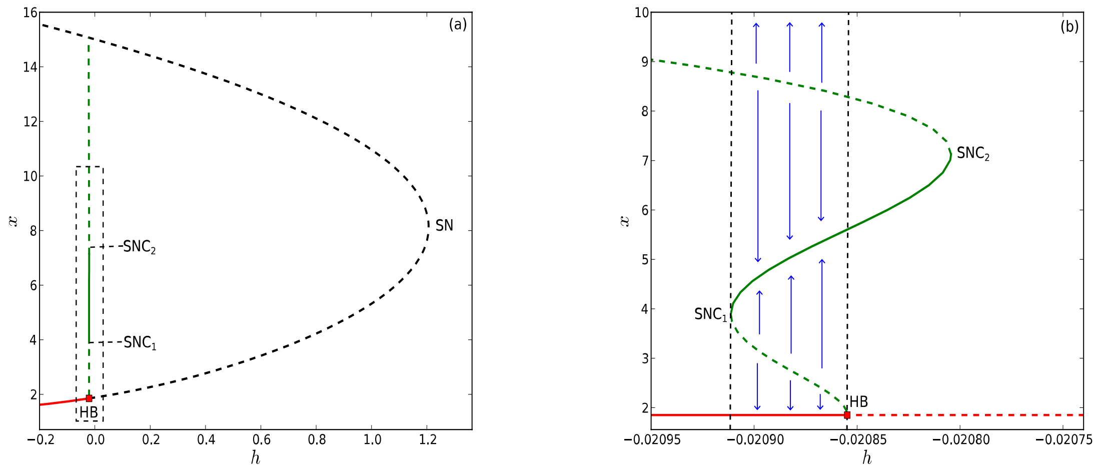

Figure 7. One-parameter bifurcation diagram of system (1.2) with respect to h. (a) h vs. x. (b) Zoomed-in part of (a).

4.5. h and g as the primary bifurcation parameters

Finally, taking the stocking or harvesting terms of both species (h) and (g) as the primary bifurcation parameters while keeping the rest of the parameter values fixed as in equation (4.1), we obtain a two-parameter bifurcation diagram that includes the supercritical (subcritical) Hopf bifurcation curve $H_s(H_u)$ (red), the saddle-node bifurcation curve SN (blue), the homoclinic bifurcation curve $Hom_i(i = 1, 2)$ (green), and the saddle-node bifurcation curve of the limit cycle SNL (cyan).

There are two Bogdanov-Takens bifurcation points: $BT_1(1.06454 \times 10^{-1}, 1.15855)$ at $h = 5.29865 \times 10^{-3}, g = -5.45824 \times 10^{-2}$ and $BT_2(8.96356, 1.45379)$ at $h = -2.33252, g = 7.04085 \times 10^{-1}$. Additionally, we identify one codimension-2 cusp point of equilibrium $CPE(5.63055, -2.09880)$ at $h = 5.00485, g = -5.96756 \times 10^{-1}$ (Note that although the ordinate value is negative, we include this point for illustration).

There are also two generalized Hopf bifurcation points: $GH_1(1.88434, 1.21781)$ at $h = -2.34637 \times 10^{-2}, g = 7.25334 \times 10^{-2}$ and $GH_2(3.17066, 1.26069)$ at $h = -1.82227 \times 10^{-1}, g = 1.72386 \times 10^{-1}$. Furthermore, a codimension-2 cusp point of the limit cycle $CPL(5.91346, 2.24578)$ is found at $h = -1.87827 \times 10^{-2}, g = 6.77107 \times 10^{-2}$, with period 3.55240×10^{1}. See Figure 8 for details.

In particular, both generalized Hopf bifurcation points GH_1 and GH_2 are connected by the saddle-node bifurcation curve of the limit cycle SNL. Most interestingly, the first homoclinic cycle branch Hom_1 from the bifurcation point BT_1 and the second homoclinic cycle branch Hom_2 from the bifurcation point BT_2 approach the same heteroclinic cycle, which connects two boundary equilibria $(0, 0)$ and $(16, 0)$. This indicates that both species may go extinct as $h = g = 0$.

Setting $\Omega_1 = \{h > 0, g > 0\}, \Omega_2 = \{h < 0, g > 0\}, \Omega_3 = \{h < 0, g < 0\}$ and $\Omega_4 = \{h > 0, g < 0\}$, we find that non-oscillatory coexistence exists in Ω_1, while both non-oscillatory and

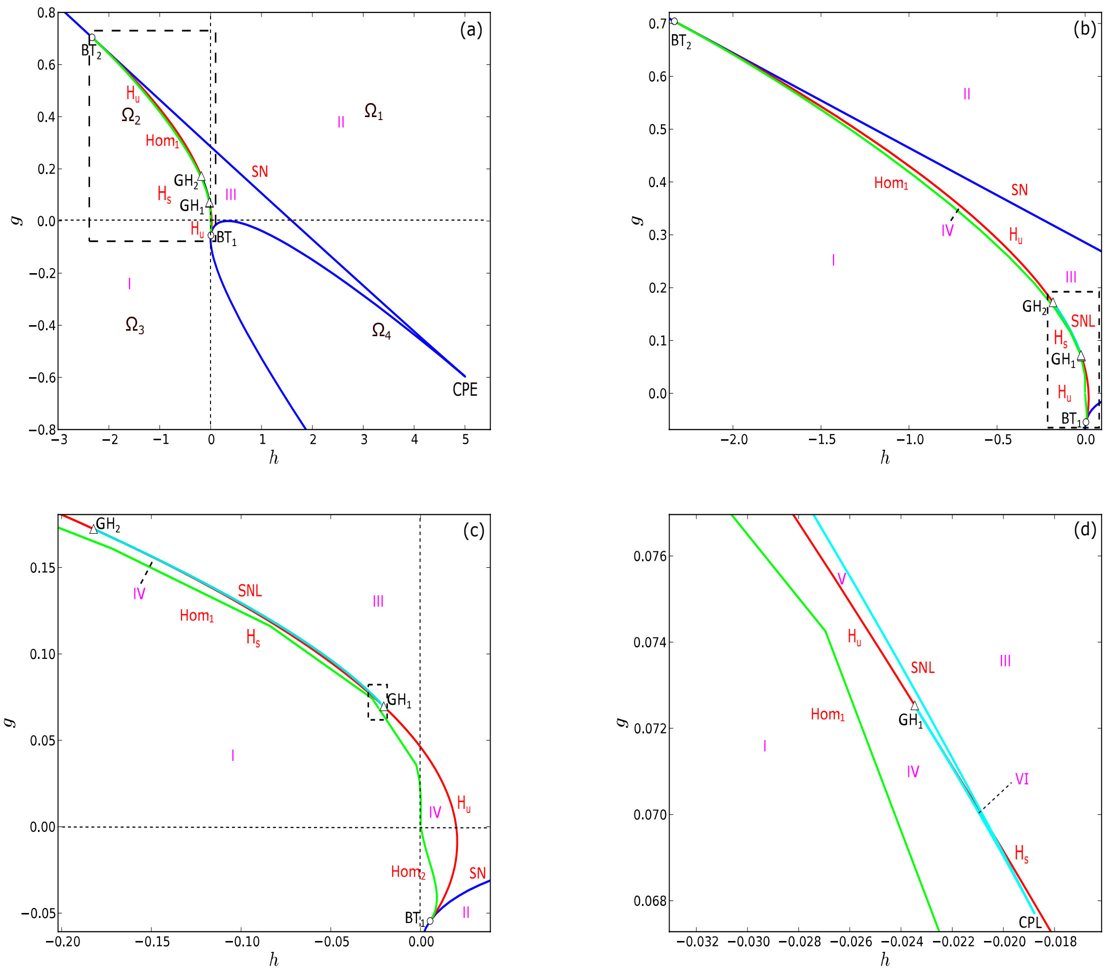

Figure 8. Two-parameter bifurcation diagram of system (1.2) with respect to h and g. (a) h vs. g. (b) First zoomed-in part of (a). (c) Second zoomed-in part of (a). (d) Third zoomed-in part of (a). Here, SN, $H_s(H_u)$, $Hom_i(i = 1, 2)$, SNL, $GH_i(i = 1, 2)$, CPE, CPL, and $BT_i(i = 1, 2)$ denote the saddle-node bifurcation curve (blue), supercritical (subcritical) Hopf bifurcation curve (red), homoclinic cycle bifurcation curve (green), saddle-node bifurcation curve of limit cycle (cyan), generalized Hopf bifurcation point, cusp of equilibrium, cusp of limit cycle, and Bogdanov-Takens bifurcation point, respectively.

oscillatory coexistence occur in the regions Ω_2 and Ω_4. Notably, no dynamics are observed in the region Ω_3, meaning that stocking both species is ineffective under the current conditions.

The bifurcation diagram is divided into six regimes: I-VI, with corresponding phase portraits as follows (See Figure 9 for details):

I: A saddle and a stable focus.

II: No positive equilibrium.

III: A saddle and an unstable focus.

IV: A saddle and a stable limit cycle containing an unstable focus.

V: A saddle and a large unstable limit cycle enclosing a small stable limit cycle, which in turn encloses an unstable focus.

VI: A saddle and three limit cycles (a large unstable limit cycle enclosing a middle stable limit cycle, which in turn encloses a small unstable limit cycle), containing a stable focus.

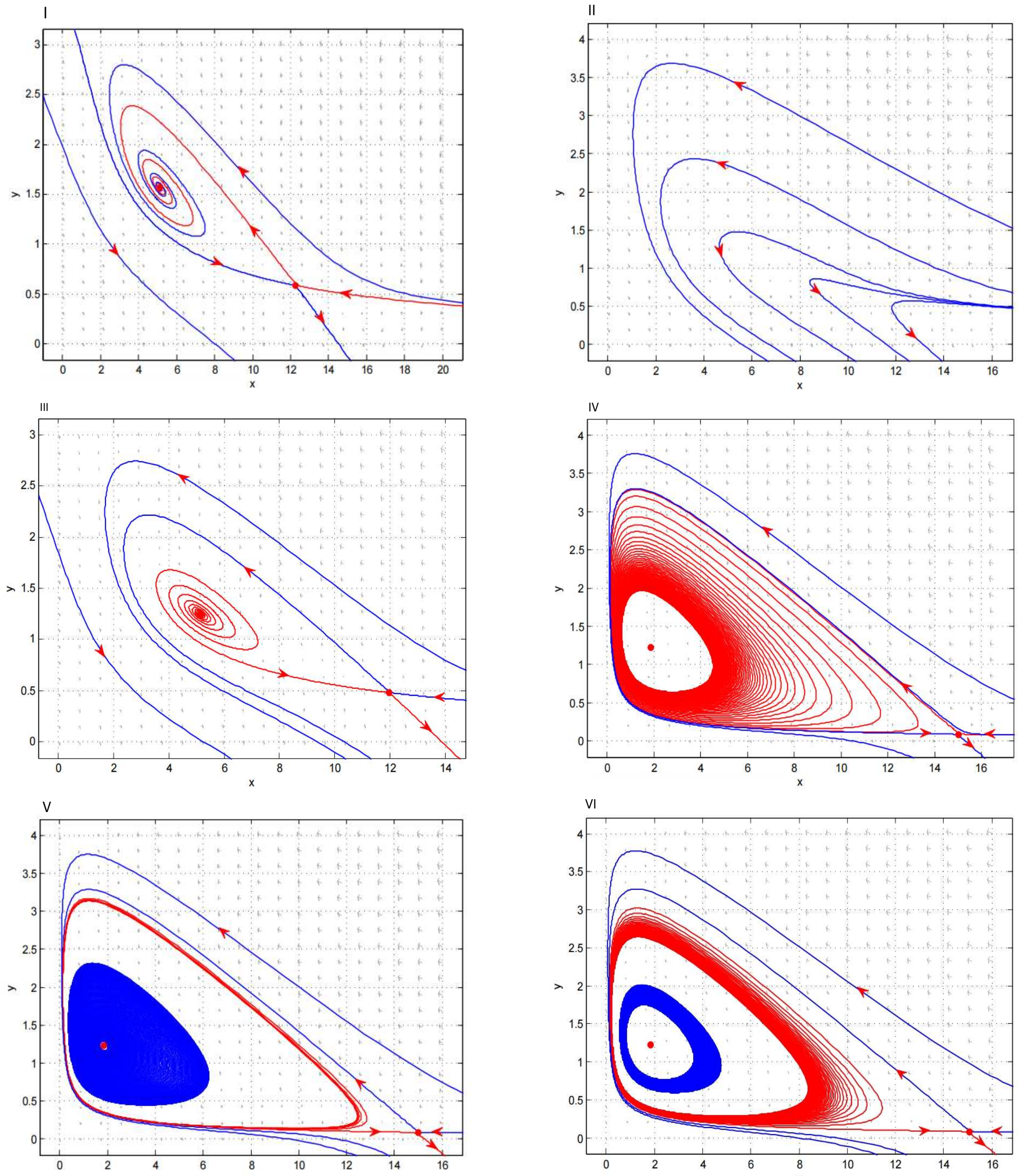

Figure 9. The corresponding phase portraits of regions I-VI in Figure 8.

This analysis suggests that, for the current system, stocking the prey while harvesting the predator may benefit the overall system. It is crucial to adopt appropriate measures to regulate the biological system, as these insights can inform conservation efforts and sustainable management strategies aimed at maintaining ecological balance and biodiversity amid anthropogenic pressures.

Remark 4.1. In Figure 8, all the homoclinic cycles in the first branch Hom_1 and the second branch Hom_2 approach the same heteroclinic cycle, which connects the two boundary equilibria

$(0,0)$ and $(16,0)$ as $h=g=0$.

5. Conclusion and discussion

In this paper, we investigate the complex dynamics of a Gause-type predator-prey system with harvesting and stocking, analyzing various bifurcations, including saddle-node bifurcation, cusp bifurcation, Hopf bifurcation of codimension at least 3, and Bogdanov-Takens bifurcation of codimension 3. Our findings highlight the crucial role of the conversion rate in determining coexistence dynamics. A low conversion rate may lead to system collapse, whereas an increasing conversion rate can promote oscillatory coexistence. The existence of a codimension-2 cusp of a limit cycle suggests the presence of two unstable limit cycles and one stable limit cycle.

Global bifurcation diagrams reveal transitions between different dynamic regimes. Interestingly, we identify two distinct Bogdanov-Takens bifurcation points, indicating that two separate homoclinic cycle branches converge at a heteroclinic cycle. The emergence of a heteroclinic cycle suggests that incorporating harvesting or stocking strategies can help prevent the collapse of the biological system. Our results indicate that stocking the prey (or predator) while harvesting the predator (or prey) can promote both non-oscillatory and oscillatory coexistence, whereas stocking both species may not benefit the system.

These findings emphasize the importance of selecting appropriate management strategies for biological systems in the context of harvesting and stocking. However, given the seasonal nature of fishing, it would be interesting to explore periodic harvesting or stocking in predator-prey systems, which we leave for future research.

Acknowledgements

The authors are grateful to the anonymous referees for their useful comments and suggestions.

A. Appendix: Coefficients in the proof of Theorem 3.2

$$
\begin{aligned}
&\overline{a}_{00}=-\omega_1,\ \overline{a}_{10}=d-amx^*,\ \overline{a}_{01}=-ax^*,\ \overline{a}_{20}=\frac{d-2amx^*}{2x^*},\ \overline{a}_{11}=-a,\\
&\overline{b}_{00}=\frac{\omega_2(d-amx^*)^2}{am}-\omega_3,\ \overline{b}_{10}=\frac{(\omega_2+m)(d-amx^*)^2}{amx^*},\\
&\overline{b}_{01}=amx^*+a\omega_2x^*-d,\ \overline{b}_{11}=a(\omega_2+m);\\
&\overline{c}_{00}=\overline{a}_{01}\overline{b}_{00}-\overline{a}_{00}\overline{b}_{01},\quad \overline{c}_{10}=\overline{a}_{11}\overline{b}_{00}-\overline{a}_{10}\overline{b}_{01}+\overline{a}_{01}\overline{b}_{10}-\overline{a}_{00}\overline{b}_{11},\\
&\overline{c}_{01}=\overline{a}_{10}-\frac{\overline{a}_{00}\overline{a}_{11}}{\overline{a}_{01}}+\overline{b}_{01},\quad \overline{c}_{20}=-\overline{a}_{20}\overline{b}_{01}+\overline{a}_{11}\overline{b}_{10}-\overline{a}_{10}\overline{b}_{11},\\
&\overline{c}_{11}=\frac{\overline{a}_{11}(\overline{a}_{00}\overline{a}_{11}-\overline{a}_{01}\overline{a}_{10})}{\overline{a}_{01}^2}+2\overline{a}_{20}+\overline{b}_{11},\quad \overline{c}_{02}=\frac{\overline{a}_{11}}{\overline{a}_{01}},\quad \overline{c}_{30}=-\overline{a}_{20}\overline{b}_{11},\\
&\overline{c}_{21}=-\frac{\overline{a}_{11}(\overline{a}_{20}\overline{a}_{01}^2+\overline{a}_{00}\overline{a}_{11}^2-\overline{a}_{01}\overline{a}_{10}\overline{a}_{11})}{\overline{a}_{01}^3},\quad \overline{c}_{12}=-\frac{\overline{a}_{11}^2}{\overline{a}_{01}^2},\\
&\overline{c}_{31}=\frac{\overline{a}_{11}^2(\overline{a}_{20}\overline{a}_{01}^2+\overline{a}_{00}\overline{a}_{11}^2-\overline{a}_{01}\overline{a}_{10}\overline{a}_{11})}{\overline{a}_{01}^4},\quad \overline{c}_{22}=\frac{\overline{a}_{11}^3}{\overline{a}_{01}^3};\\
&\overline{d}_{00}=\overline{c}_{00},\quad \overline{d}_{10}=\overline{c}_{10}-\overline{c}_{00}\overline{c}_{02},\quad \overline{d}_{01}=\overline{c}_{01},\quad \overline{d}_{20}=\overline{c}_{00}\overline{c}_{02}^2-\frac{\overline{c}_{10}\overline{c}_{02}}{2}+\overline{c}_{20},
\end{aligned}
$$

$$\overline{d}_{11}=\overline{c}_{11},\quad \overline{d}_{30}=\frac{1}{2}(\overline{c}_{10}-2\overline{c}_{00}\overline{c}_{02})\overline{c}_{02}^{2}+\overline{c}_{30},\quad \overline{d}_{21}=\frac{\overline{c}_{02}\overline{c}_{11}}{2}+\overline{c}_{21},$$
$$\overline{d}_{12}=2\overline{c}_{02}^{2}+\overline{c}_{12},\quad \overline{d}_{40}=\frac{1}{4}\overline{c}_{02}(4\overline{c}_{00}\overline{c}_{02}^{3}+(\overline{c}_{20}-2\overline{c}_{02}\overline{c}_{10})\overline{c}_{02}+2\overline{c}_{30}),$$
$$\overline{d}_{31}=\overline{c}_{02}\overline{c}_{21}+\overline{c}_{31},\quad \overline{d}_{22}=-\overline{c}_{02}^{3}+\frac{3\overline{c}_{12}\overline{c}_{02}}{2}+\overline{c}_{22};$$
$$\overline{e}_{00}=\overline{d}_{00},\quad \overline{e}_{10}=\overline{d}_{10},\quad \overline{e}_{01}=\overline{d}_{01},\quad \overline{e}_{20}=\overline{d}_{20}-\frac{\overline{d}_{00}\overline{d}_{12}}{2},\quad \overline{e}_{11}=\overline{d}_{11},\quad \overline{e}_{30}=\overline{d}_{30}-\frac{\overline{d}_{10}\overline{d}_{12}}{3},$$
$$\overline{e}_{21}=\overline{d}_{21},\quad \overline{e}_{40}=\frac{1}{4}\overline{d}_{00}\overline{d}_{12}^{2}-\frac{\overline{d}_{20}\overline{d}_{12}}{6}+\overline{d}_{40},\quad \overline{e}_{31}=\frac{\overline{d}_{11}\overline{d}_{12}}{6}+\overline{d}_{31},\quad \overline{e}_{22}=\overline{d}_{22};$$
$$\overline{f}_{00}=\overline{e}_{00},\quad \overline{f}_{10}=\overline{e}_{10},\quad \overline{f}_{01}=\overline{e}_{01},\quad \overline{f}_{20}=\overline{e}_{20},\quad \overline{f}_{11}=\overline{e}_{11},$$
$$\overline{f}_{30}=\overline{e}_{30}-\frac{\overline{e}_{00}\overline{e}_{22}}{3},\quad \overline{f}_{21}=\overline{e}_{21},\quad \overline{f}_{40}=\overline{e}_{40}-\frac{\overline{e}_{10}\overline{e}_{22}}{4},\quad \overline{f}_{31}=\overline{e}_{31};$$
$$\overline{g}_{00}=\overline{f}_{00},\quad \overline{g}_{10}=\overline{f}_{10}-\frac{\overline{f}_{00}\overline{f}_{30}}{2\overline{f}_{20}},\quad \overline{g}_{01}=\overline{f}_{01},\quad \overline{g}_{20}=\frac{9\overline{f}_{00}\overline{f}_{30}^{2}}{16\overline{f}_{20}^{2}}+\overline{f}_{20}-\frac{3(5\overline{f}_{10}\overline{f}_{30}+4\overline{f}_{00}\overline{f}_{40})}{20\overline{f}_{20}},$$
$$\overline{g}_{11}=\overline{f}_{11}-\frac{\overline{f}_{01}\overline{f}_{30}}{2\overline{f}_{20}},\quad \overline{g}_{30}=\frac{\overline{f}_{10}(35\overline{f}_{30}^{2}-32\overline{f}_{20}\overline{f}_{40})}{40\overline{f}_{20}^{2}},$$
$$\overline{g}_{21}=\overline{f}_{21}-\frac{3(20\overline{f}_{11}\overline{f}_{20}\overline{f}_{30}+\overline{f}_{01}(16\overline{f}_{20}\overline{f}_{40}-15\overline{f}_{30}^{2}))}{80\overline{f}_{20}^{2}},\quad \overline{g}_{40}=\frac{\overline{f}_{10}\overline{f}_{30}(16\overline{f}_{20}\overline{f}_{40}-15\overline{f}_{30}^{2})}{64\overline{f}_{20}^{3}},$$
$$\overline{g}_{31}=\frac{7\overline{f}_{11}\overline{f}_{30}^{2}}{8\overline{f}_{20}^{2}}+\overline{f}_{31}-\frac{5\overline{f}_{21}\overline{f}_{30}+4\overline{f}_{11}\overline{f}_{40}}{5\overline{f}_{20}};\quad \overline{h}_{00}=\overline{g}_{00},\quad \overline{h}_{10}=\overline{g}_{10},\quad \overline{h}_{01}=\overline{g}_{01}-\frac{\overline{g}_{00}\overline{g}_{21}}{\overline{g}_{20}},$$
$$\overline{h}_{20}=\overline{g}_{20},\quad \overline{h}_{11}=\overline{g}_{11}-\frac{\overline{g}_{10}\overline{g}_{21}}{\overline{g}_{20}},\quad \overline{h}_{31}=\overline{g}_{31}-\frac{\overline{g}_{21}\overline{g}_{30}}{\overline{g}_{20}};\quad \overline{j}_{00}=\overline{h}_{31}^{\frac{4}{5}}\overline{h}_{20}^{-\frac{7}{5}}\overline{h}_{00},\quad \overline{j}_{10}=\overline{h}_{31}^{\frac{2}{5}}\overline{h}_{20}^{-\frac{6}{5}}\overline{h}_{10},$$
$$\overline{j}_{01}=\overline{h}_{31}^{\frac{1}{5}}\overline{h}_{20}^{-\frac{3}{5}}\overline{h}_{01},\quad \overline{j}_{11}=\overline{h}_{20}^{-\frac{2}{5}}\overline{h}_{31}^{-\frac{1}{5}}\overline{h}_{11}.$$

References

[1] R. I. Bogdanov, *Versal deformations of a singular point of a vector field on the plane in the case of zero eigenvalues*, Funct. Anal. Appl., 1975, 9(2), 144–145.

[2] R. I. Bogdanov, *Bifurcation of the limit cycle of a family of plane vector field*, Sel. Math. Sov., 1984, 1, 373–387.

[3] F. Brauer and A. C. Soudack, *Stability regions and transition phenomena for harvested predator-prey systems*, J. Math. Biol., 1979, 7(4), 319–337.

[4] F. Brauer and A. C. Soudack, *Stability regions in predator-prey systems with constant-rate prey harvesting*, J. Math. Biol., 1979, 8(1), 55–71.

[5] F. Brauer and A. C. Soudack, *Constant-rate stocking of predator-prey systems*, J. Math. Biol., 1981, 11(1), 1–14.

[6] F. Brauer and A. C. Soudack, *Coexistence properties of some predator-prey systems under constant rate harvesting and stocking*, J. Math. Biol., 1982, 12(1), 101–114.

[7] S. Chen, J. Wei and J. Zhang, *Dynamics of a diffusive predator-prey model: The effect of conversion rate*, J. Dyn. Differ. Equ., 2018, 30(4), 1683–1701.

[8] G. Dai and M. Tang, *Coexistence region and global dynamics of a harvested predator-prey system*, SIAM J. Appl. Math., 1998, 58(1), 193–210.

[9] E. J. Doedel, A. R. Champneys, F. Dercole, T. F. Fairgrieve, Y. A. Kuznetsov, B. Oldeman, R. C. Paffenroth, B. Sandstede, X. J. Wang and C. H. Zhang, *AUTO-07P: Continuation and Bifurcation Software for Ordinary Differential Equations*, Concordia University, 2007.

[10] R. M. Etoua and C. Rousseau, *Bifurcation analysis of a generalized Gause model with prey harvesting and a generalized Holling response function of type III*, J. Diff. Eqs., 2010, 249(9), 2316–2356.

[11] W. L. Hogarth, J. Norbury, I. Cunning and K. Sommers, *Stability of a predator-prey model with harvesting*, Ecological Modelling, 1992, 62(1–3), 83–106.

[12] S. B. Hsu, *On global stability of a predator-prey system*, Math. Biosci., 1978, 39(1–2), 1–10.

[13] Y. Lamontagne, C. Coutu and C. Rousseau, *Bifurcation analysis of a predator-prey system with generalised Holling type III functional response*, J. Dyn. Differ. Equ., 2008, 20(3), 535–571.

[14] S. Laurin and C. Rousseau, *Organizing center for the bifurcation analysis of a generalized Gause model with prey harvesting and Holling response function of type III*, J. Diff. Eqs., 2011, 251(10), 2980–2986.

[15] C. Li, J. Li and Z. Ma, *Codimension 3 BT bifurcations in an epidemic model with a nonlinear incidence*, Discrete Contin. Dyn. Syst. Ser. B, 2015, 20(4), 1107–1116.

[16] C. Li and C. Rousseau, *A system with three limit cycles appearing in a Hopf bifurcation and dying in a homoclinic bifurcation: The cusp of order 4*, J. Diff. Eqs., 1989, 79(1), 132–167.

[17] Y. Liu, X. Feng, S. Ruan and J. Yu, *Periodic dynamics of a single species model with seasonal Michaelis-Menten type harvesting, II: Existence of two periodic solutions*, J. Diff. Eqs., 2024, 388, 253–285.

[18] R. M. May, J. R. Beddington, C. W. Clark, S. J. Holt and R. M. Laws, *Management of multispecies fisheries*, Science, 1979, 205(4403), 267–277.

[19] M. R. Myerscough, B. F. Gray, W. L. Hogarth and J. Norbury, *An analysis of an ordinary differential equation model for a two-species predator-prey system with harvesting and stocking*, J. Math. Biol., 1992, 30(4), 389–411.

[20] G. Peng, Y. Jiang and C. Li, *Bifurcations of a Holling-type II predator-prey system with constant rate harvesting*, Int. J. Bifurc. Chaos, 2009, 19(08), 2499–2514.

[21] L. Perko, *Differential Equations and Dynamical Systems*, Springer Science & Business Media, 2013.

[22] N. Sarif and S. Sarwardi, *Analysis of Bogdanov-Takens bifurcation of codimension-2 in a Gause-type model with constant harvesting of both species and delay effect*, J. Biol. Syst., 2021, 29(03), 741–771.

[23] F. Takens, *Forced Oscillations and Bifurcations*, Springer, 1974.

[24] D. Xiao and L. S. Jennings, *Bifurcations of a ratio-dependent predator-prey system with constant rate harvesting*, SIAM J. Appl. Math., 2005, 65(3), 737–753.

[25] D. Xiao and S. Ruan, *Bogdanov-Takens bifurcations in predator-prey systems with constant rate harvesting*, Fields Inst. Commun., 1999, 21, 493–506.

[26] Y. Xu, Y. Yang, F. Meng and S. Ruan, *Degenerate codimension-2 cusp of limit cycles in a Holling-Tanner model with harvesting and anti-predator behavior*, Nonlinear Anal. Real World Appl., 2024, 76, 103995.

[27] Y. Yang, F. Meng, Y. Xu and L. Rong, *Complex dynamics induced by additive Allee effect in a Leslie-Gower predator-prey model*, Discrete Contin. Dyn. Syst. Ser. B, 2024, 29(8), 3471–3511.

[28] Y. Yang, Y. Xu, L. Rong and S. Ruan, *Bifurcations and global dynamics of a predator-prey mite model of Leslie type*, Stud. Appl. Math., 2024, 152(4), 1–54.

[29] H. Zhang and M. Zhu, *Population dynamics of a logistic model incorporating harvesting pulses on a growing domain*, Commun. Nonlinear Sci. Numer. Simul., 2025, 146, 108768.

[30] Z. Zhang, T. Ding, W. Huang and Z. Dong, *Qualitative Theory of Differential Equations*, Amer. Math. Soc., 1992.

[31] C. Zhu and L. Kong, *Bifurcations analysis of Leslie-Gower predator-prey models with nonlinear predator-harvesting*, Discrete Contin. Dyn. Syst. Ser. S, 2017, 10(5), 1187–1206.

Received May 2025; Accepted October 2025; Available online September 2026.